JACS
JOURNAL OF THE AMERICAN CHEMICAL SOCIETY
pubs.acs.org/JACS
Perspective

Atom Transfer Radical Polymerization: A Mechanistic Perspective

Francesca Lorandi, Marco Fantin, and Krzysztof Matyjaszewski*

Cite This: https://doi.org/10.1021/jacs.2c05364
Read Online

ABSTRACT: Since its inception, atom transfer radical polymerization (ATRP) has seen continuous evolution in terms of the design of the catalyst and reaction conditions; today, it is one of the most useful techniques to prepare well-defined polymers as well as one of the most notable examples of catalysis in polymer chemistry. This Perspective highlights fundamental advances in the design of ATRP reactions and catalysts, focusing on the crucial role that mechanistic studies play in understanding, rationalizing, and predicting polymerization outcomes. A critical summary of traditional ATRP systems is provided first; we then focus on the most recent developments to improve catalyst selectivity, control polymerizations via external stimuli, and employ new photochemical or dual catalytic systems with an outlook to future research directions and open challenges.

1. INTRODUCTION

The highly reactive and elusive nature of radicals has long challenged chemists who strive to control reactivity and selectivity to maximize the yield of desired reaction products or to make functional materials.[1] In order to prepare well-defined, functional polymer materials by radical polymerization, it is necessary to develop an approach to control the growth of propagating radicals. One of the most powerful, versatile, and scalable methods for controlling (macro)molecular radical reactivity is the reversible transfer of a halogen atom to propagating radicals, forming dormant species.[2] This process is the foundation of atom transfer radical polymerization (ATRP).[3]

For over 25 years, ATRP has been used to make polymers with predetermined molecular weight (MW), low dispersity (Đ; i.e., narrow MW distribution), functionality, and architecture. ATRP has experienced an incessant evolution in terms of catalyst and reaction design, becoming one of the most prominent examples of catalysis in polymer chemistry. This Perspective begins by providing a brief historical background of the ATRP development, followed by highlighting recent advances in the design of ATRP catalysts and methods. The focus is on the critical role that mechanistic studies play in affirming ATRP as an efficient and sustainable technique for the synthesis of functional polymers.

From a mechanistic point of view, ATRP is rooted in atom transfer radical addition (ATRA)[4] and inspired by metal catalyzed telomerizations and redox initiated polymerizations.[3a,5] In contrast to telomerizations, where polymer MW does not increase with monomer conversion, in a typical ATRP, the polymer MW increases linearly with conversion, retaining low Đ and indicating that all chains grow concurrently.[6] ATRP kinetics follow the principle of the "persistent radical effect" (PRE).[7] According to the PRE, if a system can generate both a persistent, stable radical (Y) and a transient radical ($R^{\bullet}$) at an equal rate, the latter is involved in self-termination events that trigger the buildup of the persistent radical concentration (Scheme 1). This guides the system toward cross-termination between persistent and transient radicals, minimizing the self-termination of transient, unstable species. In ATRP, the persistent radical is an oxidized metal catalyst termed the "deactivator", while the corresponding reduced metal catalyst is the "activator" (vide infra).

Scheme 1. General Scheme of the Persistent Radical Effect[a]

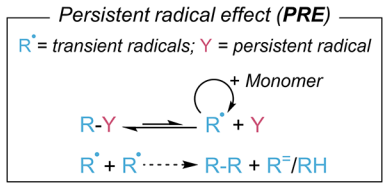

[a]R−R and R=/RH indicate termination via radical combination and radical disproportionation, respectively.

The concept of activation/deactivation that is at the core of ATRP derives from ATRA. Transition metal-catalyzed ATRA was developed in the 1960s to add an alkyl halide across a C═C double bond.[4,8] Cu complexes are the most common ATRA catalysts.[9] The mechanism of Cu-catalyzed ATRA involves the halogen atom abstraction from an alkyl halide (RX) substrate by a Cu^{I}/L complex (L = ligand, Scheme 2a). During this "activation" step, the Cu^{I} species undergoes an inner sphere electron transfer (ISET), resulting in the generation of a halogenated X−Cu^{II}/L complex and an organic transient radical.[4,10] The latter adds to an alkene, and the resulting radical monoadduct is deactivated by halogen atom abstraction from the X−Cu^{II}/L deactivator complex. To maximize the monoadduct yield, (i) radical deactivation must be fast, keeping radical concentration relatively low to minimize termination events; (ii) the rate of deactivation must

Scheme 2. General Mechanisms of Cu-Catalyzed (a) ATRA, (b) normal ATRP, and (c) ATRP with Continuous (Re)generation of the $Cu^{I}L^{+}$ Activator[a]

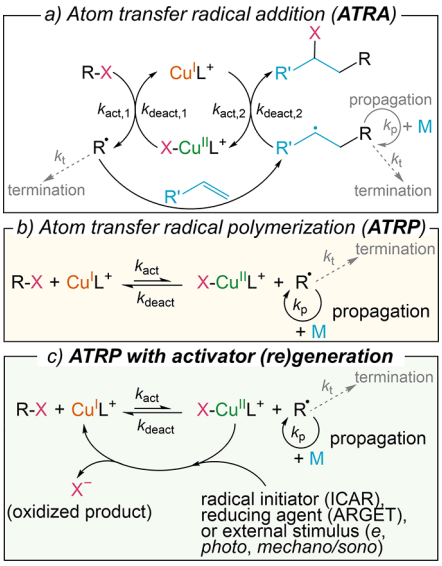

[a]The parameters k_{act}, k_{deact}, k_t, and k_p indicate the rate constants of activation, deactivation, radical termination, and propagation, respectively.

be greater than the rate of alkene propagation to prevent the formation of oligomers/polymers. Further activation of the product is generally avoided by employing substrates that form inactivated monoadducts.

ATRP is based on a similar mechanism of radical activation/deactivation as that of ATRA; however, the (macro)radicals generated upon the addition of monomer molecules are susceptible to further activation. In Cu-catalyzed ATRP, the activator $Cu^{I}L^{+}$ (L is typically a polydentate amine ligand) reacts with the RX initiator or dormant species through a concerted ISET and halogen atom transfer to form propagating radicals and the deactivator $X-Cu^{II}L^{+}$ (Scheme 2b).[10,11] Radical propagation occurs until radical chain ends are deactivated by $X-Cu^{II}L^{+}$, forming X-capped dormant species and regenerating $Cu^{I}L^{+}$. The rate constant of activation of dormant species is typically much smaller than the rate constant of radical deactivation, i.e., $k_{act} \ll k_{deact}$. Thus, the ATRP equilibrium is shifted toward dormant species. As a consequence, the relatively low concentration of propagating radicals (10^{-7}–10^{-9} M) limits the occurrence of termination reactions, which typically involve <10% of the total amount of growing chains.

According to the PRE, unavoidable terminations cause the accumulation of the "persistent radical" $X-Cu^{II}L^{+}$, which leads to a progressive slow down and ultimately halts the polymerization. Therefore, to reach high monomer conversion, ATRP was originally conducted using a stoichiometric amount of catalyst and RX initiator. The relatively low activity of seminal Cu complexes toward C−X bonds required high catalyst loadings (1 mol % or 10 000 ppm relative to monomer concentration) and relatively harsh polymerization conditions, which could preclude the widespread utilization of ATRP. Similarly, ATRA initially saw limited adoption in organic synthesis, largely due to the need for >10 mol % catalyst relative to the substrate to obtain the desired product with acceptable yield.

The development of methods for continuous (re)generation of the $Cu^{I}L^{+}$ activator in ATRP and their subsequent implementation in ATRA represented a major breakthrough, enabling a drastic reduction in catalyst concentrations.[4,12] In ATRP with activator (re)generation (Scheme 2c), air-stable Cu^{II} salts are employed and reduced in situ to Cu^{I} species, simplifying the reaction handling.[12b,13] The accumulation of the "persistent radical" $X-Cu^{II}L^{+}$ is counteracted by its continuous reduction to Cu^{I} species, thus avoiding rate retardation. Therefore, the loading of Cu catalysts can be reduced to <100 and even <10 ppm. This was facilitated by the identification and design of new ligands for more active Cu catalysts, guided by mechanistic analysis and computational approaches.[14]

Historically, the first ATRP with activator (re)generation was obtained by introducing metallic Cu into the system and exploiting the comproportionation reaction between Cu^{0} and Cu^{II}/L species to form $Cu^{I}L^{+}$.[15] This method was termed supplemental activator and reducing agent (SARA) ATRP, upon recognizing that Cu^{0} was also capable of activating dormant species, although to a much lower extent in comparison to $Cu^{I}L^{+}$.[16] Other compounds, including ascorbic acid and tin(II) 2-ethylhexanoate, were explored as reducing agents to continuously reduce the $X-Cu^{II}L^{+}$ deactivator via activator regenerated by electron transfer (ARGET) ATRP.[13b,17] Similarly, thermal radical initiators, e.g., azobisisobutyronitrile, were employed to generate radicals during the polymerization to induce the continuous (re)generation of $Cu^{I}L^{+}$ in the so-called initiators for continuous activator regeneration (ICAR) ATRP.[17] The ARGET and ICAR methods were also implemented in ATRA, enabling one to achieve a high yield of the desired monoadducts using ≤100 ppm of Cu catalyst.[18]

The (re)generation of the ATRP activator can also be achieved through external stimuli such as light, electrical current/potential, and ultrasound in the presence or absence of piezoelectric materials, as in *photo*ATRP,[19] *e*ATRP,[20] and *mechano/sono*ATRP,[21] respectively. These systems use mild conditions and offer the possibility to temporally and spatially control polymerizations by regulating the applied stimulus.[22] Temporal control is also achievable in ARGET[23] and SARA ATRP.[24] The design and use of more active ATRP catalysts provided more effective temporal control, while potentially enabling one to expand the scope of monomers and functional groups.[25] ATRP systems with activator (re)generation can tolerate the presence of some amounts of oxygen. When one adjusted the reaction volume to diminish the headspace as well as judiciously selected the ratios between the various ATRP components, it was possible to obtain well-controlled polymerizations without deoxygenation.[26] Robust oxygen-tolerant ATRP was recently developed by means of enzymatic degassing,[27] via light irradiation combined with sodium pyruvate in photoinduced ICAR (PICAR) ATRP,[28] or by modulating electrical currents in the presence of sodium pyruvate in *e*ATRP.[29]

These advances were made possible by an in-depth investigation of the ATRP mechanism and by defining expressions and correlations to predict ATRP outcomes. The next section of this Perspective discusses the fundamental characteristics of an ATRP catalyst, namely, its ability to activate dormant species and deactivate propagating radicals and its selectivity toward these processes. The aim is to highlight the importance of the deactivation step and of the

https://doi.org/10.1021/jacs.2c05364
J. Am. Chem. Soc. XXXX, XXX, XXX−XXX

side reactions, aspects that are commonly overlooked relative to the activation step when designing new catalysts. The subsequent sections describe key advancements in externally controlled ATRP enabled by the improved understanding of related mechanistic features. Relevant comparisons with ATRA are included because of the common underlying mechanism and therefore the possibility to reciprocally inspire future developments. The final outlook explores some remaining challenges and describes strategies to enhance the versatility of ATRP and atom transfer radical processes.

2. ACTIVITY AND SELECTIVITY OF ATRP CATALYSTS

2.1. Activation of Dormant Species. In a normal ATRP process without activator (re)generation, the polymerization rate (R_p) is approximately fixed by the initial ratio of [Cu^IL^+] to [X−$Cu^{II}L^+$], according to eq 1, where K_{ATRP} is the ATRP equilibrium constant and [M] is the monomer concentration.

$$R_p = k_p[M][R^\bullet] = k_p K_{ATRP}\frac{[RX][Cu^IL^+][M]}{[X{-}Cu^{II}L^+]} \quad (1)$$

To speed up a normal ATRP with seminal low-activity complexes (L = 2,2,-bipyridine, bpy), it was necessary to raise the reaction temperature or pressure[30] or to employ more active catalysts. However, the latter could result in a very high radical concentration at the beginning of the process, leading to large fractions of terminated chains and thus poor initiation efficiency and low chain-end functionality.

Conversely, the kinetics of ATRP with activator regeneration follows the steady state in radical concentration, similar to free radical polymerization and reversible addition−fragmentation chain-transfer (RAFT) polymerization.[12b,31] As a result, the radical concentration is (i) directly proportional to the square root of the rate of Cu^IL^+ regeneration, $R_{Cu^IL^+regeneration}$, and (ii) inversely proportional to the square root of the rate constant of radical termination, k_t (eq 2). Therefore, R_p is virtually independent of the catalyst loading, which can be very low, and the rate determining step is the reduction of the Cu^{II} deactivator. This opened new possibilities for tuning the polymerization rate by varying the nature and/or amount of the reducing agent, radical initiator, or external stimuli.

$$[R^\bullet] = \sqrt{\frac{R_{Cu^IL^+regeneration}}{k_t}} \quad (2)$$

Moreover, high catalyst activity that was detrimental in normal ATRP became advantageous if combined with a Cu^I regeneration pathway.[12b,25] More active ATRP catalysts have higher K_{ATRP}. The latter determines the equilibrium molar ratio between the X−$Cu^{II}L^+$ deactivator and Cu^IL^+ activator (eq 1); thus, highly active catalysts result in higher fractions of the deactivator, improving the control (cf. eq 3 and the related discussion). Cu complexes with tris(2-pyridylmethyl)amine (TPMA) and tris[2-(*N*,*N*-dimethylamino)ethyl]amine (Me_6TREN) as ligands (Figure 1a) were used for ATRP with activator (re)generation down to ∼10 ppm loading. The same complexes enabled the catalyst loading to decrease in intramolecular ATRA (i.e., atom transfer radical cyclization, ATRC)[4] using 5−100 ppm of Cu/TPMA with AIBN in an ICAR-type process.

TPMA and Me_6TREN, tetradentate tripodal ligands, replaced bi-, tri-, and linear tetra-dentate ligands (e.g., bpy, *N*,*N*,*N*′,*N*″,*N*″-pentamethyldiethylenetriamine, PMDETA, and

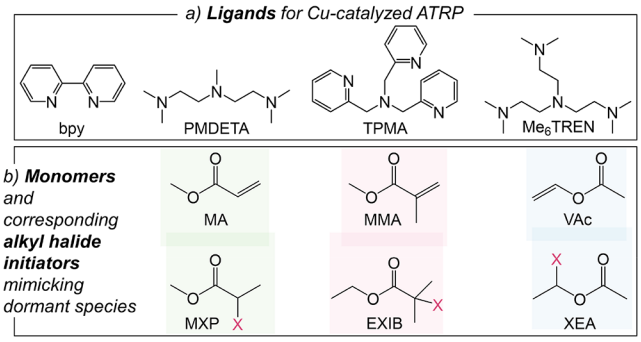

Figure 1. (a) Common ligands for Cu complexes used as ATRP catalysts and (b) monomers mentioned in this Perspective with the alkyl halide (X = Cl, Br) initiators that mimic the corresponding dormant species in ATRP.

N,*N*,*N*′,*N*″,*N*‴,*N*‴-hexamethylenetetramine, HMTETA) that form Cu complexes with much lower ATRP activity. TPMA and Me_6TREN have very often been employed as ligands in ATRP for over 20 years, favored by their commercial availability and high activity of the corresponding Cu complexes (K_{ATRP} = 9.6 × 10^{-6} for Cu/TPMA and 1.5 × 10^{-4} for Cu/Me_6TREN, measured in acetonitrile at 22 °C using ethyl α-bromoisobutyrate, EBiB, as the initiator, Figure 1b). Cu/TPMA is particularly suitable for ATRP in water, thanks to its stability over a broad range of pH and low tendency of Cu^ITPMA^+ to disproportionate.[32] It is also the catalyst of choice for ATRP in dispersed aqueous media, as it strongly interacts with anionic surfactants forming ion pairs that promote the polymerization control.[33] The 15-times higher activity of Cu/Me_6TREN in comparison to Cu/TPMA makes it the preferred catalyst in organic solvents, where RX activation is 2−3 orders of magnitude slower than in water.[25]

The design of novel ligands for Cu complexes with even higher ATRP activity has been the focus of intense research.[12b] This was mainly motivated by the possibilities to diminish the catalyst loading to the ppm or subppm level and to expand the monomer scope of ATRP, further strengthened by recent studies revealing that more active catalysts are beneficial to reduce the extent of side reactions and to improve temporal control over polymerizations.[25] The ATRP activity of a Cu complex can be inferred from the value of the standard reduction potential (E^θ) of the X−$Cu^{II}L^+$/X−Cu^IL couple, which is approximately equal to its half-wave potential, $E_{1/2}$(X−$Cu^{II}L^+$/X−Cu^IL). In fact, a linear relationship exists between $E_{1/2}$(X−$Cu^{II}L^+$/X−Cu^IL) and log K_{ATRP} for a fixed RX, solvent, and temperature (Figure 2). Thus, one of the most explored strategies to design ligands for Cu complexes with high ATRP activity consists of introducing electron-donating groups (EDGs) in the ligand structure to shift $E_{1/2}$(X−$Cu^{II}L^+$/X−Cu^IL) to more negative values. EDGs increase the coordination strength of the ligand to the Cu^{II} center relative to the Cu^I center. This diminishes the energy needed for the electron transfer in ATRP activation; therefore, K_{ATRP} increases. It should be noted that K_{ATRP} values are defined not only by $E_{1/2}$(X−$Cu^{II}L^+$/X−Cu^IL) but also by the halidophilicity of Cu^{II} species (cf. eq 4).[34]

The modification of TPMA by EDGs in para (*p*) position on pyridine rings has led to the most active Cu catalysts reported to date (Figure 3).[35] Cu complexes with TPMA-based ligands having dimethylamino ($TPMA^{NMe2}$) and pyrrolidine ($TPMA^{pyr}$) *p*-substituents exhibited 4 and 9 orders of

https://doi.org/10.1021/jacs.2c05364
J. Am. Chem. Soc. XXXX, XXX, XXX−XXX

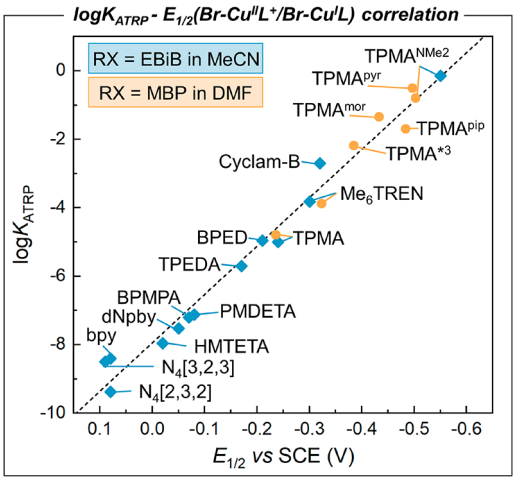

Figure 2. Linear correlation between $E_{1/2}$(Br−Cu^{II}L^{+}/Br−Cu^{I}L) (reported versus the saturated calomel electrode, SCE) and the corresponding log K_{ATRP} determined for EBiB in acetonitrile (blue diamonds) and MBP in DMF (orange dots). L acronyms are reported for each point. Ligands and initiators' structures are depicted in Figures 1 and 3 and in ref 14a.

magnitude higher K_{ATRP} values in comparison to those of Cu/TPMA and Cu/bpy, respectively. These ligands are readily accessible through the synthesis of tris(4-chloro-2-pyridylmethyl)amine (TPMA^{3Cl}), followed by the replacement of electron-withdrawing Cl atoms with the desired EDG.[35b] $E_{1/2}$ of Cu complexes with TPMA-based ligands decreases with the increase of the ED character of the *p*-substituents (Figure 3). The latter can be correlated to the Hammett parameter (σ_p)[36] or the nucleophilicity parameter (N).[37] Both of these parameters are tabulated for a broad range of functional groups; therefore, they can be used to guide the design of new ligands and predict the activity toward C−X bonds of the resulting Cu complexes.

The design of Cu complexes that surpass the activity of Cu/TPMA^{NMe2} and Cu/TPMA^{pyr} was computationally explored.[38] The rigidification of ligand caps in nitrogen-based ligands shortened the Cu−N$_{cap}$ distance (Figure 4), diminishing the stability of the highest occupied molecular orbital (HOMO), thus favorably affecting the ΔG of the electron transfer and of the overall ATRP process. As a result, Cu complexes with rigid piperidine or quinuclidine analogues of TPMA^{NMe2} (pip^{NMe2} and quin^{NMe2}, Figure 4) should exhibit 3−4 orders of magnitude higher activity than Cu/TPMA^{NMe2}. However, the

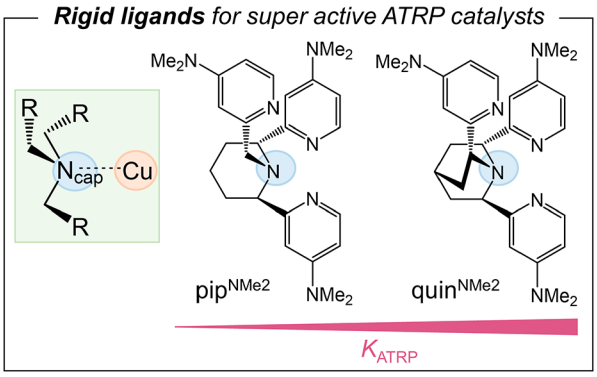

Figure 4. Schematics of N$_{cap}$−Cu coordination for tripodal ligands used in ATRP and structures of rigid piperidine and quinuclidine analogous of TPMA^{NMe2} (pip^{NMe2} and quin^{NMe2}, respectively).

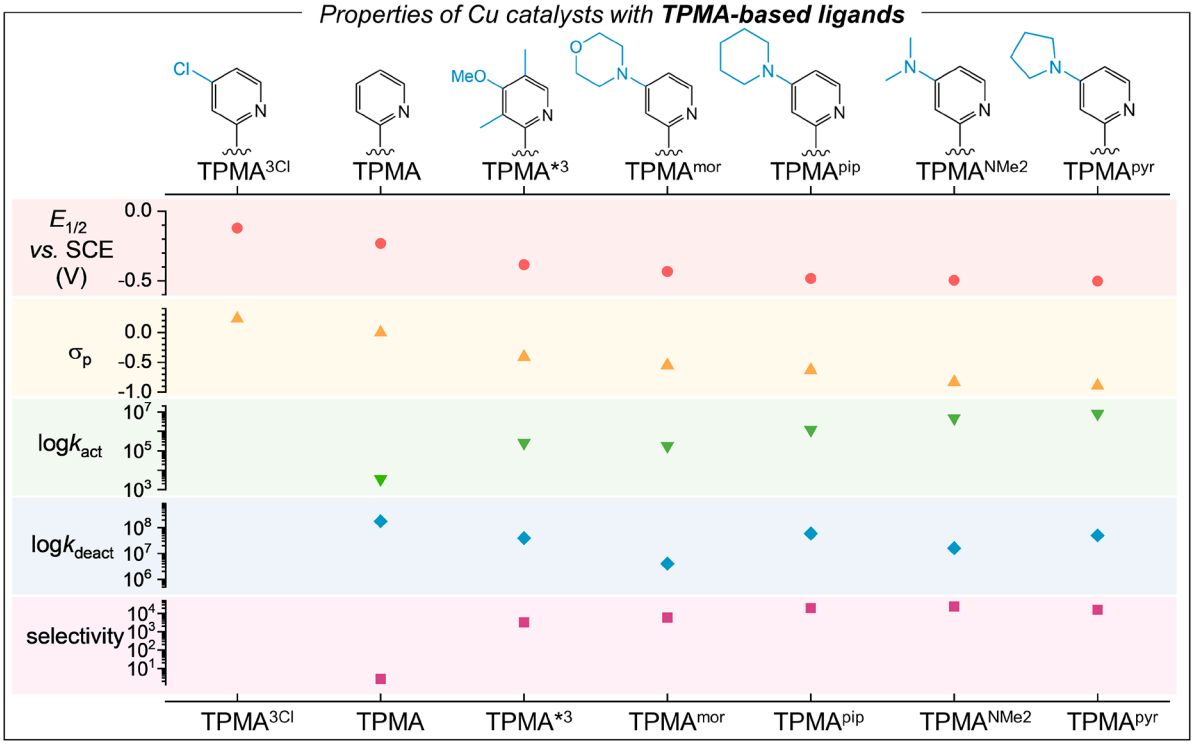

Figure 3. Trends in Cu complexes with TPMA-based ligands used as ATRP catalysts as a function of the *p*-substituents on the pyridine rings: variation of $E_{1/2}$(Br−Cu^{II}L^{+}/Br−Cu^{I}L), Hammett parameter (σ_p), activation and deactivation rate constants (k_{act} and k_{deact}, respectively), and selectivity toward ATRP (see eq 7).

https://doi.org/10.1021/jacs.2c05364
J. Am. Chem. Soc. XXXX, XXX, XXX−XXX

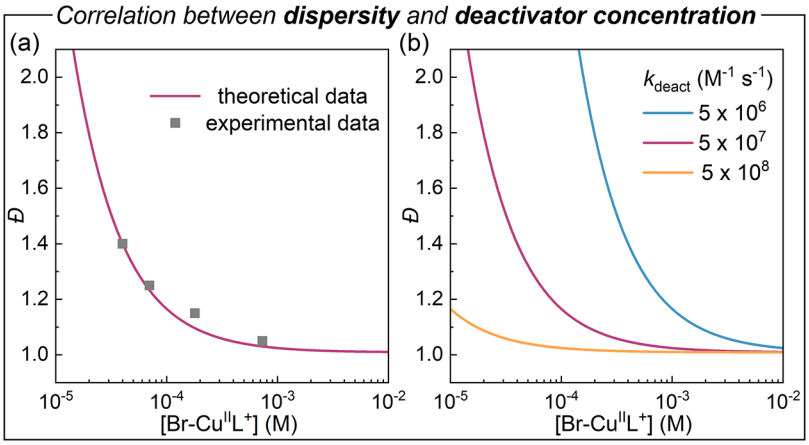

Figure 5. (a) Variation of Đ as a function of the equilibrium concentration of Br−Cu^{II}Me$_6$TREN$^+$ for the ATRP of MA (50 vol % in DMSO) at room temperature. In this system, k_{deact} = 5.6 × 10^7 M^{-1} s^{-1} and K_{ATRP} = 7 × 10^{-5};[44] thus, at equilibrium, >99% of the catalyst is in the deactivator form (i.e., [Br−Cu^{II}L$^+$] ≈ [CuBr$_2$/L]$_0$). Dots correspond to real-case polymerizations in ref 43c. Curves were obtained using eq 3 with fixed p = 76%, DP$_n$ = 150, and k_p = 13 100 M^{-1} s^{-1}.[45] (b) Variation of Đ as a function of k_{deact} in an otherwise identical system.

synthesis of these ligands is not trivial. The replacement of a methylene group in the quinuclidine cap with an oxygen could offer an easier synthetic pathway without compromising the activity of the resulting Cu catalyst.[39]

According to computational data, these rigidified Cu complexes can unlock the ATRP of less activated monomers such as vinyl acetate (VAc), *N*-vinylpyrrolidone, and *N*-vinylformamide. K_{ATRP} values correlate to the free energy of C−X bond dissociation (BDFE) in RX initiators mimicking dormant species.[14a,40] K_{ATRP} is ca. 6 orders of magnitude lower for 1-bromoethyl acetate (BEA; Figure 1b, VAc mimic) than for methyl 2-bromopropionate (MBP; Figure 1b; methyl acrylate: MA mimic). This gap in reactivity matches the predicted gain in K_{ATRP} when replacing Cu/Me$_6$TREN with Cu/quin^{NMe2}. Thus, the ATRP of VAc catalyzed by Cu/quin^{NMe2} should proceed in a similar manner to the ATRP of a typical acrylate monomer catalyzed by Cu/Me$_6$TREN. However, the rigidity of the ligand may affect the deactivation of propagating radicals and the selectivity of the catalyst. Both aspects must be critically evaluated when designing new ligands.

2.2. Deactivation of Propagating Radicals. In ATRP, the deactivation rate constant k_{deact} defines the control over chain growth. Đ is proportional to the ratio of k_p to k_{deact} and inversely proportional to the deactivator concentration, according to eq 3, where p is the monomer conversion and DP$_n$ is the degree of polymerization. Equation 3 is valid in the case of fast initiation and negligible contributions of transfer and termination.

$$Đ = \frac{M_w}{M_n} = 1 + \frac{1}{DP_n} + \left(\frac{k_p[RX]_0}{k_{deact}[X{-}Cu^{II}L^+]}\right)\left(\frac{2}{p} - 1\right) \quad (3)$$

The value of k_{deact} is generally ≫k_{act} and close to the diffusion limit for a second-order reaction, which shifts the ATRP equilibrium toward the dormant species. Contrary to k_{act}, k_{deact} is only slightly affected by the nature of the ligand and its substituents (Figure 3) as well as by the reaction conditions, such as solvent polarity and temperature. The parameters affecting k_{deact} are still only partially understood.[14a] Over an order of magnitude lower k_{deact} values were measured for some of the most active complexes (e.g., Cu/TPMA^{mor}, Cu/TPMA^{NMe2}) with respect to classical Cu/TPMA and Cu/Me$_6$TREN, which exhibit k_{deact} > 10^7−10^8 M^{-1} s^{-1} for Br-based systems.[35b] The halogen nature has an important effect on k_{deact}, as chlorine and, to a greater extent, fluorine atoms strongly bind to Cu^{II}, stabilizing the deactivator. This results in a decrease in k_{deact} and thus a less effective polymerization control.[41] On the other hand, iodides have poor affinity for Cu^{II} species.[14a,41] Therefore, Br is the preferred chain-end functionality in ATRP when a large k_{deact} is needed.

Tuning the rate of radical deactivation allows for the preparation of polymers with tunable Đ values. While RDRPs are classically used to prepare polymers with low dispersity, the possibility to control the breadth and shape of polymer MW distribution by RDRP has recently attracted great attention.[42] Đ can be increased by decreasing the concentration of the Cu^{II} deactivator (cf. eq 3).[43] Figure 5a compares experimental and theoretical Đ values for PMA prepared by *photo*ATRP with different initial concentrations of CuBr$_2$/Me$_6$TREN.[43c] Experimental Đ values ranged from 1.05 to 1.40 by decreasing the loading of CuBr$_2$/Me$_6$TREN from 7.3 × 10^{-4} to 4.0 × 10^{-5} M. The theoretical Đ values were calculated from eq 3 and matched the experimental data. Figure 5b shows the variation in PMA dispersity as a function of k_{deact}. If Cu/Me$_6$TREN is replaced with a catalyst that has similar activity but 1 order of magnitude lower k_{deact}, high Đ = 1.8 is already obtained at a catalyst loading of ∼2.0 × 10^{-4} M.

The concentration of the X−Cu^{II}L$^+$ deactivator in ATRP depends on the ATRP equilibrium and on the halidophilicity constant K_X^{II} that expresses the affinity of Cu^{II}L^{2+} for X$^-$ according to eq 4.

$$K_X^{II} = \frac{[X{-}Cu^{II}L^+]}{[X^-][Cu^{II}L^{2+}]} \quad (4)$$

Typical Cu catalysts have K^{II}_{Br} ≈ 10^4−10^7 M^{-1} in organic solvents and K^{II}_{Br} < 10^2 in aqueous media.[32] Therefore, aqueous ATRP generally requires one to employ a large excess of halide ions relative to the Cu^{II} loading to prevent the dissociation of X−Cu^{II}L$^+$ that results in increased polymer dispersity (cf. eq 3). However, the proper amount of X$^-$ depends on the particular aqueous system: Methacrylate monomers typically require a >50-fold excess of X$^-$ to obtain polymers with relatively low Đ,[32,46] while lower amounts could

https://doi.org/10.1021/jacs.2c05364
J. Am. Chem. Soc. XXXX, XXX, XXX−XXX

be used for acrylates,[47] although the reason behind this different behavior needs to be further investigated.

Another key feature of a well-controlled polymerization is the preservation of chain-end functionalities to prepare block copolymers and other architectures and to make polymers amenable to postpolymerization modifications. The chain-end functionality (CEF) of a polymer can be expressed as CEF = 1 − DCF, where DCF corresponds to the fraction of dead chains. In ATRP, DCF is calculated as the ratio of the concentration of terminated chains [T] to the initial concentration of the initiator ($[RX]_0$, eq 5). For systems with a very small contribution of termination (ca. < 5%), DCF is proportional to k_t, the target degree of polymerization (DP_T), and monomer conversion and inversely proportional to the polymerization time t, initial monomer loading ($[M]_0$), and ${k_p}^2$.

$$\mathrm{DCF} = 1 - \mathrm{CEF} = \frac{[\mathrm{T}]}{[\mathrm{RX}]_0} = \frac{2\mathrm{DP_T}k_t[\ln(1-p)]^2}{{k_p}^2 t[\mathrm{M}]_0} \quad (5)$$

On the basis of eq 5, the ATRP of MA at room temperature with DP_T = 100 can be conducted to 80% conversion in less than 10 min with only 2% of terminated chains (Table 1).[48]

Table 1. DCF as a Function of the Polymerization Time Needed to Reach 80% Conversion for Different Monomers[a]

monomer[b]	T (°C)	10 min	1 h	24 h	1 week
methyl methacrylate	25	>50%	>50%	19% (18 mM)	3% (2.5 mM)
methyl acrylate	25	2% (1.6 mM)	<1% (0.3 mM)	<1% (11 μM)	<1% (1.6 μM)
oligo(ethylene glycol) methyl ether methacrylate	25	>50%	16% (0.7 mM)	<1% (30 μM)	<1% (4 μM)

[a]The molar concentration of dead chains is in parentheses; it is equal to the amount of reducing agent needed to regenerate the Cu^IL^+ activator. [b]Conditions: DP_T = 100. Hypothetical bulk polymerizations for methyl (meth)acrylate; [oligo(ethylene glycol) methyl ether methacrylate] = 0.42 M in water. DCF calculated according to eq 5.

However, for methyl methacrylate (MMA) under similar conditions, the polymerization time must be extended to hours, mostly due to the slower propagation of methacrylate radicals, so higher temperatures can be beneficial to improve CEF. For a bulky methacrylate monomer such as oligo(ethylene glycol) methyl ether methacrylate (OEOMA), which has a relatively low k_t and is typically polymerized in diluted aqueous solutions (10−20 wt % monomer), the DCF is <1% for a polymerization time of 24 h.

Importantly, DCF does not correlate to polymer Đ, so it is possible to obtain high CEF even for polymers with a high Đ. When eq 5 was applied to the *photo*ATRPs in Figure 5a, DCF was in all cases ≪10%, even for PMA with Đ > 1.4. According to eq 3, polymer Đ is predominantly affected by the ratio of the rates of propagation and deactivation processes: rapidly propagating monomers tend to add more units before being deactivated; thus, efficient deactivation is needed to obtain a low Đ. On the other hand, DCF is proportional to $k_t/(k_p)^2$ (eq 5); therefore, rapid monomer propagation can be beneficial to achieve high CEF. In addition, CEF increases with a decrease in the polymerization rate, which is primarily dictated by the rate of deactivator regeneration.[31] For acrylate monomers, the high $(k_p)^2/k_t$ favors high CEF.

By rearranging eq 5, one can calculate the concentration of terminated chains [T] at a given polymerization time. In ATRP, one molecule of deactivator is accumulated for every terminated chain. With activator (re)generation, the accumulated $X{-}Cu^{II}L^+$ is reduced to Cu^I species by employing, for instance, a suitable reducing agent in an ARGET ATRP process. Therefore, the value of [T] in eq 5 corresponds to the equivalents of reducing agent needed to regenerate the Cu^I activator from $X{-}Cu^{II}L^+$ that builds up upon radical termination (see values in parentheses in Table 1). It should be noted that, in real polymerization systems, k_t values strongly depend on chain length and viscosity (i.e., conversion); thus, the contribution of termination processes decreases with conversion.

The most active ATRP catalysts have k_{act} and k_{deact} values that approach the diffusion limit for second order reactions (ca. 10^9 M^{-1} s^{-1}, depending on solvent viscosity). The most active catalysts to date exhibit $k_{act} \approx 10^7$ M^{-1} s^{-1} for MA-mimicking dormant species in DMF at room temperature.[35b] However, these catalysts have lower k_{deact} values compared to less active complexes. Therefore, the goal in catalyst design should shift from enhancing their activity to improving their ability to deactivate propagating radicals and their selectivity toward ATRP activation/deactivation.

2.3. Selectivity. Transition metal complexes can be employed to control the propagation of radicals via formation/dissociation of organometallic species, as in organometallic mediated radical polymerization (OMRP).[49] Cobalt complexes are the most employed in OMRP.[49a] The ATRP activator Cu^IL^+ can also react with propagating radicals to form organocupric intermediates $R{-}Cu^{II}L^+$ (Scheme 3). The latter participates in a radical activation/deactivation (i.e., homolytic cleavage of $R{-}Cu^{II}L^+$/capture of $R^\bullet$ by Cu^IL^+) equilibrium typical of an OMRP. The OMRP equilibrium constant, K_{OMRP}, is defined as the ratio between the rate constants of activation

Scheme 3. General Mechanism of ATRP with Activator Regeneration, Including the Formation of Organocupric Intermediates That Participate in the OMRP Equilibrium and in CRT

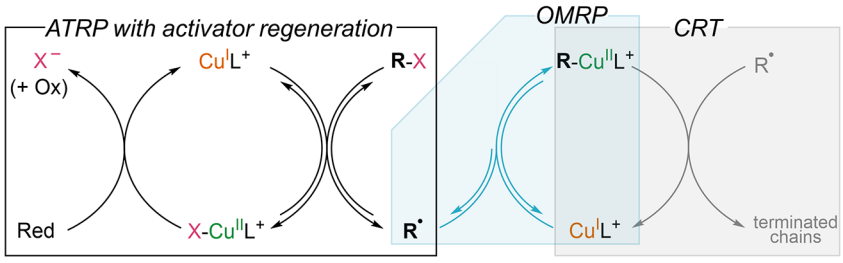

https://doi.org/10.1021/jacs.2c05364
J. Am. Chem. Soc. XXXX, XXX, XXX−XXX

and deactivation of propagating radicals ($k_{act,OMRP}/k_{deact,OMRP}$, eq 6). On one hand, organometallic intermediates can improve polymerization control due to the fast reversible formation of R−$Cu^{II}L^+$. However, the paramagnetic R−$Cu^{II}L^+$ can rapidly react with propagating radicals producing terminated chains and regenerating Cu^IL^+ in a process called Cu-catalyzed radical termination (CRT).[50]

$$K_{OMRP} = \frac{k_{act,OMRP}}{k_{deact,OMRP}} = \frac{[R^\bullet][Cu^IL^+]}{[R{-}Cu^{II}L^+]} \quad (6)$$

The elusive nature of organometallic species is hampering precise quantifications of their effect in ATRP.[51] The selectivity of a catalyst for the ATRP vs OMRP process can be expressed as the relative tendency of Cu^IL^+ to react with either dormant species (ATRP activation) or propagating radicals (OMRP deactivation). Therefore, the selectivity can be defined as the ratio of ATRP activation rate to the OMRP deactivation rate (eq 7). The selectivity of a Cu complex is directly proportional to the concentration of RX and inversely proportional to the equilibrium amount of propagating radicals. Therefore, when one targets lower DP (i.e., higher $[RX]_0$) and performs slower polymerizations (i.e., lower $[R^\bullet]$), the result is improved selectivity toward ATRP. Interestingly, the catalyst selectivity is independent of its concentration, but it increases with an increase in its ATRP activity. The OMRP deactivation between Cu^IL^+ and $R^\bullet$ is generally fast with $k_{deact,OMRP}$ approaching the diffusion limit for a second order reaction for many catalysts.[51a]

$$\text{selectivity} = \frac{R_{act}}{R_{deact,OMRP}} = \frac{k_{act}[RX][Cu^IL^+]}{k_{deact,OMRP}[R^\bullet][Cu^IL^+]} = \frac{k_{act}[RX]}{k_{deact,OMRP}[R^\bullet]} \quad (7)$$

Values of $k_{deact,OMRP}$ and $k_{act,OMRP}$ have been determined by electrochemical and spectrochemical studies and by simulations of Cu/L + RX systems.[51] According to these studies, the electronic and steric properties of the ligand affect the ATRP equilibrium much more than the OMRP equilibrium. No clear correlation exists between the ATRP and OMRP activity of typical Cu catalysts employed in ATRP, although all Cu complexes with TPMA-based ligands bearing ED *p*-substituents showed lower $k_{deact,OMRP}$ and $k_{act,OMRP}$ values in comparison with those of Cu/TPMA.[51a] When eq 7 was applied to these complexes, Cu/TPMA was determined to be less selective, while the most active ATRP catalysts were more selective (Figure 3). The polymerization solvent showed a larger impact on k_{act} than on OMRP rate constants. The effect of the polymerization temperature on the OMRP parameters has yet to be explored, and little is known about the role of the chain length of propagating radicals.

The selectivity of a Cu/L complex is important to evaluate the impact of CRT. In ATRP with tertiary radicals as well as styrene and acrylonitrile radicals, CRT can generally be neglected.[51a] However, for acrylate species, CRT can dominate over conventional radical termination (RT), accounting for up to 90% of the terminated chains.[52] The rate constant of CRT is weakly affected by the catalyst nature. Nevertheless, simulations of ATRP systems showed that, if the catalyst activity is increased, the equilibrium concentration of Cu^IL^+ decreases; thus, organocupric intermediates are diminished, and the contribution of CRT becomes negligible versus RT (Figure 6).[51a]

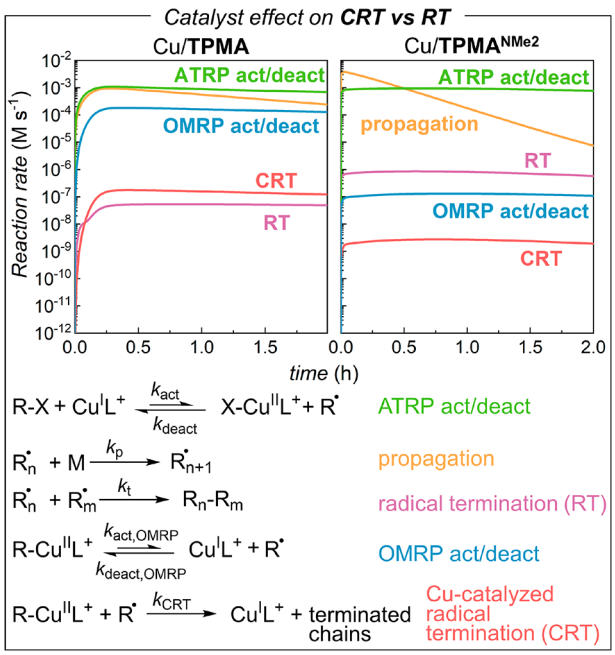

Figure 6. PREDICI simulations of ARGET ATRP of MA in DMF, catalyzed by 200 ppm of $CuBr_2$/TPMA or $CuBr_2$/$TPMA^{NMe2}$. Adapted from ref 51a. Copyright 2019 American Chemical Society.

Besides reacting with RX or radicals, Cu^IL^+ can disproportionate to $Cu^{II}L^{2+}$ and Cu^0 + L. Disproportionation is faster in polar solvents, particularly in water.[32] Solvents and ligands that preferentially stabilize Cu^{2+} over Cu^+ favor disproportionation.[35b] TPMA strongly stabilizes both Cu^+ and Cu^{2+}, providing an active catalyst that is very stable toward disproportionation, thus being the catalyst of choice in aqueous ATRP.[32] Overall, Cu^I complexes with amine ligands are excellent catalysts to activate alkyl halides; however, the reactivity of Cu^IL^+ with $R^\bullet$ (OMRP-CRT) and with itself (disproportionation) must be considered to design the most selective catalytic systems.

3. ELECTROCATALYSIS IN ATRP

In recent years, there has been a renewed interest in powering organic synthesis by electrochemical methods, encouraged by the increasing availability of renewable electricity that can be harnessed to sustainably produce value-added chemicals.[53] The concerted atom and *electron* transfer at the core of ATRP and ATRA motivated the attempts of triggering these processes by electrochemical means. Electrochemically mediated ATRP (*e*ATRP) was developed in 2011 for the controlled polymerization of acrylates in organic solvents[20] and then extended to several monomers and solvents, including aqueous systems.[54] In contrast, reports on electrochemically triggered ATRA or ATRC reactions are scarce.[55] In the field of polymer science, *e*ATRP is a pioneering process that inspires the implementation of electrochemical stimuli in cationic,[56] ring-opening,[57] and RAFT[58] polymerizations.

In *e*ATRP, the deactivator X−$Cu^{II}L^+$ is reduced at the surface of a working electrode (WE) by applying a constant potential (E_{app}) or current (I_{app}) in a potentiostatic or galvanostatic setup, respectively. The electro-reduction gen-

https://doi.org/10.1021/jacs.2c05364
J. Am. Chem. Soc. XXXX, XXX, XXX−XXX

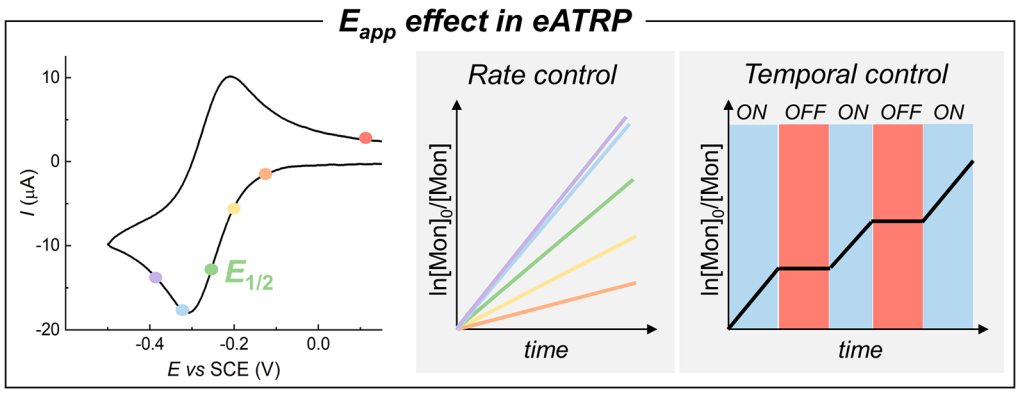

Figure 7. Exemplified effect of applied potential E_{app} on the polymerization kinetics in *e*ATRP. Colored dots on the voltammograms correspond to the different E_{app} values, and they are color-coded with the kinetic lines and with the time interval of the ON/OFF periods.

erates X−Cu^{I}L that partially dissociates to X^{-} and the activator Cu^{I}L^{+}. An important advantage of *e*ATRP is that the value of E_{app} determines the relative molar ratio of the oxidized and reduced catalyst species at the electrode's surface, according to the Nernst equation (eq 8, where R is the gas constant, T is temperature, and F is Faradays' constant), and thus the ratio of ATRP deactivator to activator. Therefore, E_{app} can be dialed to tune the polymerization rate (Figure 7) as well as the polymerization control ($Đ$ is affected by the concentration of X−Cu^{II}L^{+}; cf. eq 3).

$$E_{app} = E_{1/2} + \frac{RT}{F}\frac{[X{-}Cu^{II}L^{+}]}{[X{-}Cu^{I}L]} \tag{8}$$

Another unique advantage of the electrochemical approach is the possibility to estimate the CEF during an *e*ATRP from the consumed electrical charge. The total charge passed during the polymerization (Q_{tot}; eq 9) corresponds to the sum of (i) the charge needed to reduce a fraction of the initial X−Cu^{II}L^{+} to Cu^{I} species (Q_{red}) and (ii) the charge required to continually reduce X−Cu^{II}L^{+} formed during the polymerization as a consequence of radical terminations (Q_{rt}).[46] The value of Q_{red} can be calculated using Faraday's law of electrolysis in eq 9, where n_{red} corresponds to the number of moles of Cu^{I} electrogenerated at the WE (which in turn depends on E_{app} and is calculated from eq 8). Thus, if $Q_{tot} > Q_{red}$, a fraction of the passed charge (Q_{rt}) was used to compensate for the termination events. The value of Q_{rt} can then be used to calculate the moles of terminated chains, n_{rt}.

$$Q_{tot} = Q_{red} + Q_{rt} = n_{red}F + n_{rt}F \tag{9}$$

*e*ATRP distinguishes itself from other ATRP methods with activator (re)generation for its strict temporal control over the polymerization. In most ATRP systems, temporal control is obtained by switching off the stimulus (e.g., light and ultrasound) or by removing the Cu wire in SARA ATRP.[21b,24,44] Similarly, in *e*ATRP, the applied current/potential can be switched off.[59] The halt of the polymerization can take a few minutes to several hours: A faster stop is obtained when more active ATRP catalysts are employed as the equilibrium concentration of Cu^{I}L^{+} is lower; thus, fewer activation events can take place in the "off" period before all Cu^{I}L^{+} is oxidized.[25] Nevertheless, in *e*ATRP, it is also possible to quickly halt the polymerization by changing the applied current/potential rather than simply turning it off.[20] If a suitable oxidizing current or potential is applied (Figure 7), Cu^{I}L^{+} is quickly converted into Cu^{II} species, stopping the polymerization in a few minutes regardless of the catalyst nature or reaction conditions. The only limitation to an instantaneous halt is the mass transport to and from the electrode. A similar concept was applied to ARGET ATRP by alternatively introducing a proper reducing or oxidizing agent.[23] However, *e*ATRP allows for a much cleaner reaction switching.

In fact, another advantage of *e*ATRP in comparison to other ATRP methods with activator (re)generation is the absence of byproducts, as electrons are the reducing agents. This is strictly true for *e*ATRPs performed in a divided cell, where the counter electrode (CE) is placed in a separated compartment with respect to the WE that is directly immersed in the polymerization solution. A simplified system (*se*ATRP) is also possible, where a sacrificial CE, typically aluminum wire, is employed in an undivided setup.[60] However, in *se*ATRP with an Al sacrificial anode, Al^{3+} ions are released in solution during polymerization, which can form complexes with typical ligands of Cu catalysts.[61] Although these Al complexes are inactive in ATRP, excess L's or buffers is needed to prevent a large decrease in the concentration of the Cu catalysts.

The adoption of electrosynthetic methods such as *e*ATRP can be hampered by the complex equipment needed. To make electrosyntheses more appealing, simpler and standardized devices were developed such as the IKA Electrasyn, where a basic potentiostat is built-in to a magnetic stirrer.[62] This simplified hardware was effectively employed for aqueous *se*ATRP under both constant applied potential or current.[62b] The availability of various accessories for running multiple *e*ATRPs in parallel, in μL volume,[63] or in flow reactors can help open new avenues for this polymerization technique. Moreover, the scale-up of *e*ATRP is facilitated by the possibility of using stainless steel reactors, whereby the reactor wall serves as the WE.[64] Finally, the electrochemical setup provides an opportunity to remove and recycle the catalyst:[65] At the end of the polymerization, a suitable potential/current is applied to reduce all Cu complexes to Cu^{0}, which deposits on the WE surface. The WE with electrodeposited Cu can then be reused for new polymerizations.

4. PHOTOCATALYZED ATRP

4.1. Beyond the Activation/Deactivation Equilibrium via Photocatalysis. The development of ATRP with activator (re)generation occurred concomitantly to a raising interest in photocatalysis for organic synthesis, following

https://doi.org/10.1021/jacs.2c05364
J. Am. Chem. Soc. XXXX, XXX, XXX−XXX

Scheme 4. General Mechanisms of *photo*ATRP Catalyzed by (a) Conventional Cu-Based ATRP Catalysts via a Reductive Quenching Path and (b) Metal-Based or (c) Organo-Photocatalysts via Oxidative Quenching

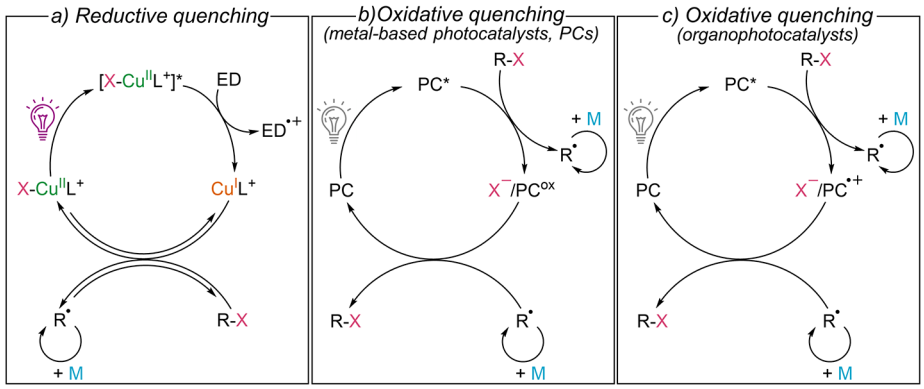

seminal reports on visible light photoredox catalysis.[66] As a consequence, light was applied to ATRP to generate radicals via photoinitiators and to trigger a catalytic activation/deactivation cycle via oxidative or reductive quenching pathways.[67]

Conventional Cu-based ATRP catalysts are employed in photochemically mediated systems (*photo*ATRP) via a reductive quenching cycle using UV or violet light to excite the $X-Cu^{II}L^+$ deactivator to $[X-Cu^{II}L^+]^*$, which is then quenched by the reaction with an electron donor (ED) (e.g., triethylamine, TEA, or free uncoordinated L).[19b,68] This reductive quenching (Scheme 4a) process generates the $Cu^{I}L^+$ activator that reacts with RX to form propagating radicals and $X-Cu^{II}L^+$ in a typical ATRP equilibrium. It was recently shown that the selection of the wavelength of light irradiation can affect the ATRP outcome in terms of polymer MW and dispersity.[69]

Alternatively, an oxidative quenching mechanism (Scheme 4b,c) is possible with suitable photocatalysts (PCs) such as Cu^{I} complexes with phenanthroline derivatives,[70] *fac*-$Ir^{III}(ppy)_3$ (ppy = 2-pyridylphenyl),[19a,71] and several families of organo-photocatalysts, e.g., phenothiazines, phenazines, and phenoxazines (Figure 8).[72] Upon photoexcitation with UV or visible light, PC* undergoes an electron transfer to the alkyl halide to generate a propagating radical and the oxidized form of the photocatalyst, PC^{ox} (for metal-based PCs) or $PC^{\bullet+}$ (for organophotocatalysts). The oxidized photocatalyst closes the catalytic cycle by deactivating the radical. A few examples of reductive quenching pathways mediated by organophotocatalysts (e.g., Eosin Y, fluorescein) in the presence of EDs were also proposed; however, they are not discussed in this Perspective.[70c,72b,73]

While photocatalytic cycles based on oxidative quenching were first developed using metal-based PCs, organocatalyzed ATRP (*o*ATRP) later dominated the field thanks to its greener character. PCs were also employed for photochemically triggered ATRA.[9,74] The latter can also proceed through an energy transfer from PC* to RX[75] rather than via electron transfer as conventionally implied for *photo*ATRP systems. In this case, the photosensitizer in its excited state transfers energy to RX, which is homolytically cleaved. The C-centered radical adds to the alkene and then is deactivated by halogen atom abstraction.

From a mechanistic point-of-view, the traditional ATRP framework is different from ATRP mediated via an oxidative-quenching photoredox cycle. For traditional Cu complexes, the

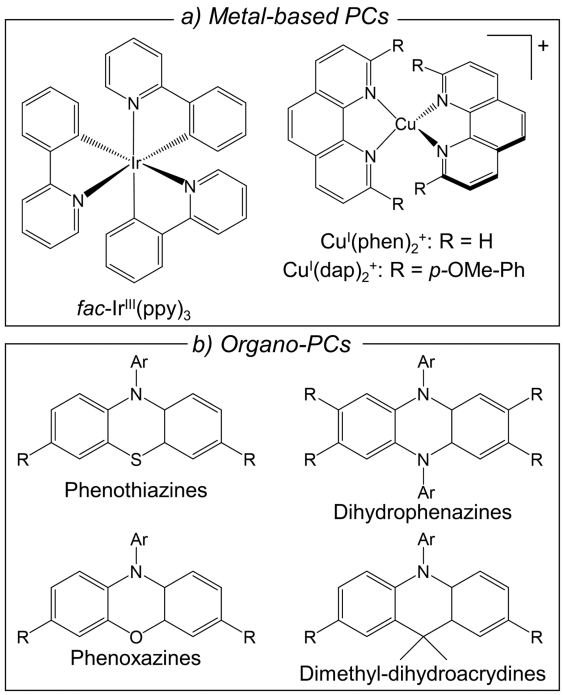

Figure 8. Structures of (a) metal-based PCs and (b) organo-PCs commonly used in *photo*ATRP and *o*ATRP, respectively.

activation energies (and thus the rate constants) of the activation and deactivation reactions are tied via the ATRP equilibrium with $K_{ATRP} = k_{act}/k_{deact}$. K_{ATRP} is generally $\ll 1$; thus, the activation energy for the activation reaction is much higher than that of the deactivation reaction (Scheme 5a). The reaction between $Cu^{I}L^+$ and RX is an ISET, which drastically lowers the activation energy of both activation and deactivation, if compared to an outer sphere electron transfer (OSET) mechanism.[10]

The mechanism of *photo*ATRP via oxidative quenching follows a different energy profile (Scheme 5b). The energy of a photon is injected into the system so that the relation $K_{ATRP} = k_{act}/k_{deact}$ does not hold. The ground state photocatalyst (PC) is promoted to an excited state (PC*); from the excited state (either singlet or triplet state), the RX activation reaction is exoergonic.[76] Fast activation of RX by PC* generates $R^{\bullet}$ and the oxidized photocatalyst PC^{ox} or $PC^{\bullet+}$, which may form a weakly bound adduct with X^- (PC^{ox}/X^- or $PC^{\bullet+}/X^-$). In the photochemical cascade, the deactivation reaction of radicals by

https://doi.org/10.1021/jacs.2c05364
J. Am. Chem. Soc. XXXX, XXX, XXX−XXX

Scheme 5. Free Energy Comparison in a Traditional ATRP and in ATRP Mediated via Photoredox Catalysis through an Oxidative Quenching Pathway

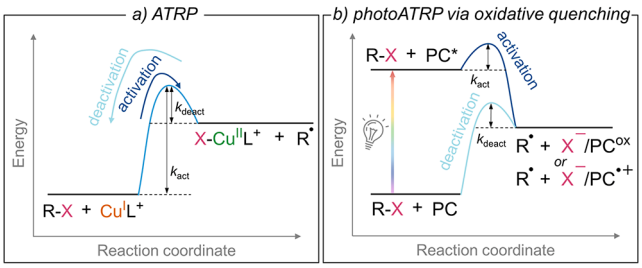

PC^{ox}/X^- or $PC^{\bullet+}/X^-$ is also exoergonic, so that fast deactivation is promoted. Even if both k_{act} and k_{deact} can be very high, the overall process can be slow because of the inefficiency of light absorption or the very short lifetime of PC* or radical cations.

The efficiency of RX activation in *photo*ATRP is typically limited by low quantum efficiency (Φ) and the short lifetime of the PC* excited state (τ_0), in agreement with eq 10, which expresses the quantum yield for ATRP activation (ψ_{act}) when occurring from an excited state.[76]

$$\psi_{act} \approx k_{act}[RX]\Phi\tau_0 \quad (10)$$

The electron transfer between PC* and RX follows an OSET. The deactivation reaction in *photo*ATRP is particularly difficult for two reasons: (i) the deactivator PC^{ox}/X^- or $PC^{\bullet+}/X^-$ is only formed following the inefficient activation reaction, so it hardly reaches high concentrations; (ii) in the case of organophotocatalysts, the deactivator is typically a rather unstable radical cation (its lifetime can be seconds to hours). The mechanism of radical deactivation in *photo*ATRP is not yet clear, and three pathways have been proposed has shown in Scheme 6: (i) deactivation by the $PC^{\bullet+}/X^-$ adduct (Scheme 6a);[77] (ii) $PC^{\bullet+}$ oxidizes X^- to $X^\bullet$, which traps the propagating radicals (Scheme 6b);[78] (ii) a termolecular reaction between $PC^{\bullet+}$, X^-, and $R^\bullet$ (Scheme 6c).[76]

The ideal photocatalyst should have the following properties: (i) high τ_0 and Φ; (ii) a very negative reduction potential of the PC^{ox}/PC^* or $PC^{\bullet+}/PC^*$ couple (<−1 V vs SCE); (iii) a stable PC^{ox} or $PC^{\bullet+}$, at least for the time scale of the polymerization process (hours); (iv) a relatively positive potential for the PC^{ox}/PC or $PC^{\bullet+}/PC$ couple between ca. 0 and +0.8 V vs SCE (a more positive potential can cause oxidation of X^-); (v) a strong interaction between PC^{ox}/X^- or $PC^{\bullet+}/X^-$ to favor a bimolecular deactivation process.

Scheme 6. General Mechanism of *o*ATRP with Different Deactivation Pathways[a]

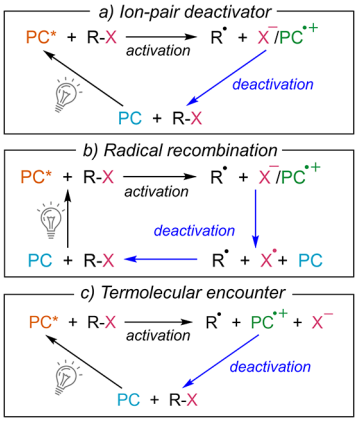

[a](a) Via formation of the $PC^{\bullet+}/X^-$ adduct; (b) via $R^\bullet$ trapping by $X^\bullet$, generated via oxidation of X^- by $PC^{\bullet+}$; (c) via a termolecular reaction.

For metal-based catalysts, the standard reduction potentials of PC^{ox}/PC^* couples for the PCs *fac*-$Ir^{III}(ppy)_3$, $Cu^I(phen)_2^+$ (phen = 1,10-phenanthroline), and $Cu^I(dap)_2^+$ (dap = 2,9-bis(*p*-anisyl)-1,10-phenanthroline) (Figure 8) are −1.73, −1.65, and −1.43 V vs SCE, respectively, in acetonitrile.[79] For comparison, the most active traditional Cu complexes barely reach −0.6 V vs SCE. The reduction potentials of the PC^{ox}/PC couples for the PC^{ox} deactivators *fac*-$Ir^{IV}(ppy)_3^+$ and $Cu^{II}(dap)_2^{2+}$ are 0.31 and 0.62 V vs SCE, respectively. Cu-based PCs with phenanthroline are largely employed in photocatalyzed ATRA,[9] where various reaction mechanisms are postulated. For instance, an ISET mechanism was proposed for certain ATRA systems catalyzed by $Cu^I(dap)_2^+$ through the formation of a Cu^{III} organometallic intermediate.[80]

For organophotocatalysts, the standard reduction potential of $PC^{\bullet+}/PC^*$ couples can be lower than −2 V vs SCE.[22] The reduction potentials of $PC^{\bullet+}/PC$ species range between 0 and 0.8 V vs SCE. For moderately oxidizing organophotocatalysts, the deactivation reaction likely proceeds through a bimolecular concerted mechanism via the formation of the $PC^{\bullet+}/X^-$ ion-pair deactivator (Scheme 6a).[78,81] This pathway is much less favorable for Cl^- ions due to the much weaker interactions with radical cations[76] and the higher tendency to undergo side reactions (e.g., H atom abstraction by $Cl^\bullet$).[22,78] Within this range of oxidation potentials, more oxidizing $PC^{\bullet+}$ provided faster deactivation. The strength of ion-pairing in $PC^{\bullet+}/Br^-$ is affected by the solvent nature with ethyl acetate and THF enhancing the association more than dimethylacetamide.[78,82] The solvent nature also impacts the quantum yield of intersystem crossing and the lifetime of the excited state activator.[82]

Several organophotocatalysts have been successfully used for the *o*ATRP of methacrylates. Conversely, well-controlled polymerization of acrylate monomers is hampered by the lower reactivity of secondary alkyl halide chain ends and by the faster propagation of secondary radicals. *o*ATRP of acrylates required to design organo-PCs simultaneously forming strongly reducing PC* for effective activation, and sufficiently oxidizing $PC^{\bullet+}$ for rapid deactivation. Dimethyl-dihydroacrydines (Figure 8) enabled the first *o*ATRP of acrylates with relatively low $Đ$.[83] The addition of LiBr further improved the control.

In addition, an electrochemical approach to *o*ATRP was devised with the purpose of enhancing the deactivation step by modulating the concentration of $PC^{\bullet+}$ via electrochemical oxidation of PC.[84] When an appropriate oxidation potential was selected, electrochemically modified *o*ATRP provided better control in the polymerization of MMA. However, more studies are needed to prove the versatility of the approach and to verify the impact of the electrochemical apparatus (e.g., the effect of the anions in the supporting electrolyte).

Besides their activation and deactivation abilities, the selectivity of PCs is equally important, albeit underexplored. Common ATRP initiators form radicals that can add to the core of dihydrophenazine PCs.[85] The resulting adducts can add to monomer species and form termination products. Moreover, these adducts have different electrochemical and

https://doi.org/10.1021/jacs.2c05364
J. Am. Chem. Soc. XXXX, XXX, XXX−XXX

photophysical properties compared to the initial PCs, affecting the *o*ATRP activation/deactivation. The sterics of PC and $R^{\bullet}$ and the solvent type play a major role in the selectivity of organophotocatalysts.[81,82]

4.2. Dual Catalysis in *photo*ATRP. Despite the improvements in *o*ATRP, *photo*ATRP with conventional Cu/L complexes shows improved polymerization control and can be performed with commercially available reagents. However, an important limitation of traditional Cu systems is the need for high-energy UV or violet light sources. To circumvent this drawback and employ visible or NIR light, dual-catalytic cycles were developed, whereby a PC is introduced into the system together with conventional Cu-based ATRP catalysts.

In dual-catalyzed *photo*ATRP, PC can be excited to PC* via visible or NIR light. Then, PC* reduces $X-Cu^{II}L^{+}$, generating $Cu^{I}L^{+}$ that can activate the RX initiator or dormant species (Scheme 7a). In some systems, PC* may be sufficiently reducing to react directly with RX generating radicals, thus offering an additional activation pathway. Conversely, the deactivation of growing chains is mediated by the Cu^{II} deactivating species, which can be used in ppm amounts. The reduction of $X-Cu^{II}L^{+}$ by PC* generates $PC^{\bullet+}$. It was proposed that Br^{-} ions formed during the ATRP activation step reduce $PC^{\bullet+}$ to the ground state PC; however, a contribution from solvent or excess L acting as ED could not be excluded.[86] An alternative is represented by "upconversion" nanoparticles as PC, harnessing their ability to absorb NIR light and emit UV light, which then excites $X-Cu^{II}L^{+}$ initiating the *photo*ATRP cycle (Scheme 7b).[87]

Scheme 7. General Mechanism of *photo*ATRP with (a) a Dual Catalyst System and (b) Upconversion Nanoparticles (UCNPs)

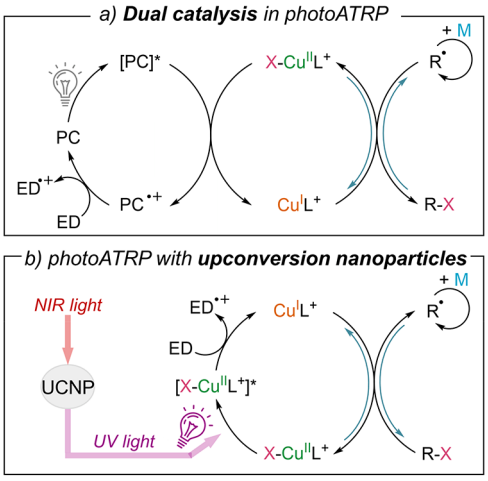

Dual catalyst systems exploited several PCs including metal porphyrins and phthalocyanines, carbon quantum dots (CQDs), covalent organic frameworks, and polyacrylonitrile-derived photoluminescent polymer assemblies under blue, green, or red light in organic solvents or aqueous media.[88] Pyridine nitrogen doped-CQDs enabled ultrafast, oxygen tolerant *photo*ATRP in water, which was exploited for 3D printing.[89] Moreover, nitrogen doped-CQDs could work under NIR light by combining them with UCNPs in composite particles.[90] Polymethine derivatives with a zwitterionic nature could be used to mediate a dual-catalyzed ATRP under NIR light.[86]

Heterogeneous PCs have the advantages of facile separation from the final polymer and recycling.[91] A smart approach to build heterogeneous PCs is to embed traditional small-molecule homogeneous PCs into a polymer network, which also allows for tuning the photophysical properties of the photocatalyst.[91b,92] Recently, a photoactive phenothiazine moiety was embedded into a conjugated microporous polymer (PTZ-CMP).[91b] The conjugated nature of the resulting network promoted light absorption in the green and red region. Therefore, PTZ-CMP was used as a heterogeneous, recyclable PC for ATRP of (meth)acrylates under green- and red-light irradiation, catalyzed by conventional Cu complexes in the presence of ED.

Most ATRP catalysts are relatively easy to reduce: Their $E_{1/2}$ ranges between 0 and −0.4 V vs SCE. For instance, the singlet excited state of zinc tetraphenylporphyrin (ZnPor*) is a suitable reductant in DMSO with a reduction potential of −0.95 V and a lifetime of 1.7 ns.[88e] A longer-living triplet excited state with high quantum yield can be generated by intersystem crossing.[93] Thus, ZnPor was effectively used in *photo*ATRP with $Br-Cu^{II}PMDETA^{+}$.[88e,93] Moreover, ZnPor* is capable of deactivating ground state oxygen via triplet−triplet annihilation, forming singlet state oxygen that is scavenged by DMSO, enabling one to perform *photo*ATRP without degassing.[88e,94]

5. MECHANO/SONO-CHEMICALLY MEDIATED ATRP

Mechanochemical forces are extensively applied in polymer chemistry to either degrade polymer chains or build macromolecules.[95] Ultrasound is a mechanochemical stimulus that creates the unusual conditions of extremely high temperatures and pressures for short periods in liquids. Ultrasound offers deeper penetration and less scattering in heterogeneous media than light irradiation. The first example of *mechano*ATRP involved the use of ultrasound together with piezoelectric $BaTiO_3$ nanoparticles to continuously reduce $X-Cu^{II}L^{+}$ via mechano-induced electron transfer[21a] The initial setup, requiring high-intensity ultrasound and high catalyst loading, was improved by employing low-intensity ultrasound and 75 ppm of Cu/TPMA.[96] With an optimized loading of 4.5 wt % $BaTiO_3$ nanoparticles, effective temporal control was achieved for ATRP of MA in DMSO. The latter could be also carried out without degassing.[97]

Strong interactions between the piezoelectric material and Cu/L catalyst can facilitate the electron transfer by decreasing the energy of the conducting band in the semiconductor. Thus, the loading of piezoelectric material was greatly decreased by replacing $BaTiO_3$ with ZnO nanoparticles,[98] which exhibited an enhanced interaction with Cu/TPMA. The reduction of $Br-Cu^{II}TPMA^{+}$ by ZnO (Scheme 8) occurred concurrently with the oxidation of excess TPMA. A small amount of radicals was generated by ultrasound-induced cavitation; however, the contribution of this process was limited. Thus, block copolymers were effectively prepared.

Nevertheless, radicals generated by ultrasound-induced cavitation can be harnessed to start and mediate polymerizations in water without adding piezoelectric compounds.[99] Thus, aqueous *sono*ATRP with a few ppm of Cu/L catalyst and low-frequency ultrasound provided well-defined (co)polymers over a broad range of MW.[99b] Effective temporal control was

https://doi.org/10.1021/jacs.2c05364
J. Am. Chem. Soc. XXXX, XXX, XXX−XXX

Scheme 8. Strategies toward Activator Regeneration in ATRP by Combining Ultrasound and Piezoelectric Materials or Carbonate Salts

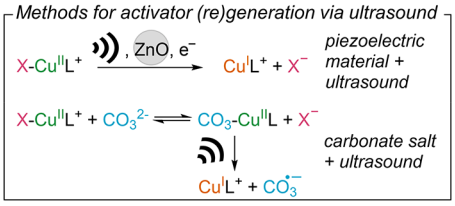

achieved thanks to the very low equilibrium concentration of Cu^IL^+ in aqueous systems with high K_{ATRP}.

The ability of ultrasound to cleave bonds can also be exploited in ATRP. Certain anions, such as carbonate and pyruvate ions, can displace Br^- from $Br-Cu^IIL^+$ complexes, forming Cu^II complexes that under selected stimuli (e.g., light, ultrasound) are homolytically cleaved to form the ATRP activator Cu^IL^+ and a radical (Scheme 8).[28a,100] Thus, the combination of Na_2CO_3 and Cu/TPMA allowed for well-controlled *sono*ATRP in organic solvents.[100]

Besides ultrasound, ball-milling can drive mechanochemical processes in sustainable solvent-free systems. Solid-state ATRP was conducted by ball-milling mixtures of solid monomers, conventional ATRP catalysts and initiators, and Cu^0 to accelerate the process.[101] Tuning the ball-milling frequency provided temporal control over polymerizations. However, mechanically induced chain scissions resulted in chain-end loss and lower MWs than expected. Nevertheless, solid-state ATRC was also demonstrated by combining ball-milling and piezoelectric $BaTiO_3$ nanoparticles.[102] At a relatively low milling frequency and TPMA amount, high yields of desired cyclic products were obtained with 5 mol % Cu^II loading.

6. OUTLOOK

The continuous development of catalysts and mechanistic approaches for ATRP provided numerous advantages including more sustainable reaction conditions, improved polymerization control, and a broader scope of monomers and functionalities. The external control of ATRP with activator (re)generation opened new avenues to manipulate the catalytic activation/deactivation cycle. The mechanistic aspects of ATRP described in this Perspective can provide new directions to overcome traditional limitations of ATRP processes, as exemplified in the following paragraphs and in Scheme 9.

6.1. Next Goals in Catalyst Design. Following the discovery of a linear correlation between the standard reduction potential of Cu complexes and their log K_{ATRP}, the design of novel ligands was aimed at preparing catalysts capable of faster RX activation. However, the efficient deactivation of propagating radicals is a key to controlling polymer dispersity, and catalyst participation in competitive equilibria (e.g., disproportionation, formation/dissociation of organocupric intermediates) can hamper the polymerization control. Therefore, the focus of mechanistic investigations and catalyst design should shift toward understanding and tuning the efficiency of deactivation and selectivity for the ATRP equilibrium. Advanced tools, such as machine learning approaches, should be used to identify new trends in the vast pool of ATRP catalysts and initiators that has been employed in the past decades. A simpler predictive tool, borrowed from organic synthesis, consists of building linear

Scheme 9. Outlook on Future Developments and Implementations of ATRP

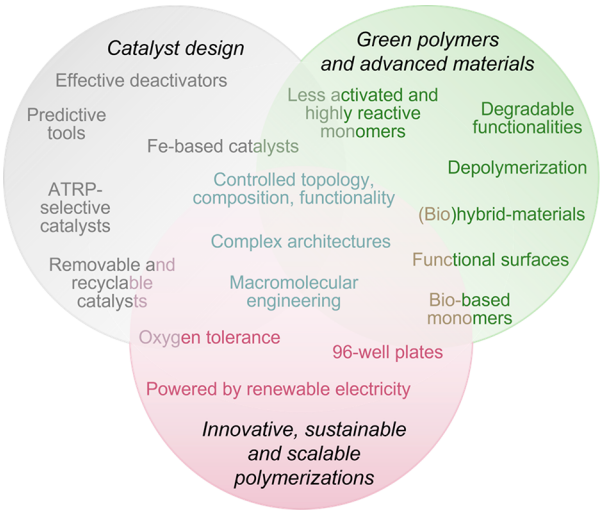

free energy relationships,[37] simultaneously treating broadly different classes of compounds to highlight relevant descriptors, while facilitating the identification of deviations from expected trends.

An enhanced understanding of the catalysts' selectivity can help one define strategies to suppress the formation of organocupric intermediates. External stimuli, such as light irradiation, currently employed to trigger polymerizations by homolytically cleaving selected chemical bonds[28a] can plausibly be directed toward R−Cu bond cleavage. On the other hand, some side reactions may be exploited to facilitate the synthesis of polymers with a complex macromolecular architecture. Indeed, the use of conditions that promoted CRT over RT enabled high conversion to be reached in the preparation of molecular bottlebrushes with densely grafted acrylate side chains via a grafting from approach,[103] since CRT provided saturated dead chains,[52b] preventing gelation caused by RT.

In addition, catalyst design should focus on easily removable and recyclable compounds to decrease the cost and improve the sustainability of ATRP. Heterogeneous catalysts may be suitable for this purpose;[91b] however, alone, they typically have reduced mobility, resulting in less efficient deactivation.[12b] Alternatively, catalysts can be removed by electrodeposition[54a] or using suitable quenching agents[104] to simultaneously halt the polymerization and precipitate the catalyst.

6.2. Fe-Catalyzed ATRP. The relatively low cost and biocompatibility of several robust Fe complexes (e.g., Fe porphyrins or simple Fe halides)[105] makes Fe-catalyzed ATRP a greener alternative to traditional ATRP with Cu catalysts.[106] In Fe-catalyzed ATRP, Fe^II species activate alkyl halide initiators or dormant chains, whereas halogenated Fe^III species deactivate propagating radicals. Fe-catalyzed ATRP has seen much narrower adoption and mechanistic scrutiny than Cu-catalyzed ATRP. This might be attributed to the enhanced contribution of side reactions, including the formation of organometallic intermediates involved in OMRP and CRT and catalytic chain transfer,[107] as well as to significant kinetic differences between Cu- and Fe-based processes. For example, anionic Cu complexes are poor ATRP catalysts, whereas anionic Fe halide species provide well-controlled ATRP even at low catalyst loadings under mild conditions.[105b,108] Correlations between thermodynamic or structural properties of Fe

https://doi.org/10.1021/jacs.2c05364
J. Am. Chem. Soc. XXXX, XXX, XXX−XXX

complexes and their ATRP activity are scarce. Fe-catalyzed ATRP can have a critical role in the sustainable production of functional polymers, and therefore, in-depth mechanistic investigations are needed to guide the design of novel Fe catalysts toward more effective and versatile polymerizations.

6.3. Unlocking Challenging Substrates and New Reactivities. One of the biggest challenges in ATRP is to broaden the scope of monomers and functionalities, including less activated monomers (e.g., VAc, vinyl chloride,[109] and even olefins[110]) and poorly reactive chain ends (e.g., -F, -N_3, isocyanate). The design of catalysts with >10^9 orders of magnitude higher K_{ATRP} than seminal ATRP catalysts could further expand the substrate scope.[40] On the other hand, relatively poor ATRP catalysts such as Cu halide salts may be suitable to regulate the propagation of highly reactive monomers (e.g., cyanoacrylates and methylene malonates). Moreover, some Cu catalysts can efficiently activate pseudohalide chain ends (e.g., dithiocarbamates); however, their reactivity does not follow the typical trends observed for alkyl halides.[111] A better understanding of their reactivity can provide ways to synergistically combine ATRP and RAFT polymerization toward more versatile systems. Dual catalytic systems often overcome the limitations of traditional catalysts.[88e] Dual systems can comprise dual polymerization mechanisms, dual catalysts, or dual stimuli. The latter can result in orthogonal reactions but also in synergistic effects. For example, in organic synthesis, the merger of photochemistry and electrochemistry unlocks previously unreachable reactivities.[112] Thus, dual systems may represent a new opportunity for expanding the scope of ATRP.

6.4. Scalable and Innovative ATRP Procedures. ATRP is an industrially relevant technique that is already used by several companies to produce specialty polymer products.[2b,113] Electrochemical ATRP can be scaled using reactor walls as electrodes[64] and electricity from renewable sources. On the other hand, polymerizations at very small scales, such as on screen printed electrodes,[63] are very important for biomacromolecules and biosensors. Electrode arrays and 96-well plates can be used for high-throughput polymerizations and screening, particularly for the development of bioconjugates and materials for bioapplications, by combining externally controlled ATRP and oxygen tolerant conditions.

6.5. Green Polymers and Advanced Materials. ATRP can be crucial in the mandatory ecological transition toward a circular plastic economy.[106,113a] Besides the development of greener polymerization systems, more efforts must be directed toward the preparation of degradable and recyclable polymers via ATRP. Therefore, it is critical to study the reactivity and eventual side reactions of various bioderived monomers and of degradable functionalities or dynamic bonds. The activation/deactivation cycle that forms the core of ATRP can also be the foundation of catalytic and controlled depolymerization processes.[114] The in-depth knowledge of the ATRP mechanism can serve as a basis to develop depolymerization systems that enable high-yield monomer recovery under scalable conditions.

Finally, the development of new catalysts and systems to trigger ATRP under mild, nontoxic conditions, coupled with the continuous study of polymerization mechanisms, offers the opportunity to design polymer- and inorganic/polymer-hybrid materials with precisely controlled features for a broad variety of applications.[115] These includes super soft materials,[116] bioconjugates and polymeric carriers for drug delivery,[117] and functionalized surfaces with lubricious, antimicrobial, or antifouling properties.[118]

As researchers continuously address these challenges and exploit these opportunities, ATRP will continue to be a valuable strategy for the synthesis of functional polymer materials for advanced technological applications. Moreover, atom transfer radical reactions for small-molecule transformations can also benefit from present and future advances in ATRP.

■ AUTHOR INFORMATION

Corresponding Author

Krzysztof Matyjaszewski − *Department of Chemistry, Carnegie Mellon University, Pittsburgh, Pennsylvania 15213, United States;* orcid.org/0000-0003-1960-3402; Email: km3b@andrew.cmu.edu

Authors

Francesca Lorandi − *Department of Chemistry, Carnegie Mellon University, Pittsburgh, Pennsylvania 15213, United States; Department of Industrial Engineering, University of Padova, 35131 Padova, Italy;* orcid.org/0000-0001-5253-8468

Marco Fantin − *Department of Chemical Sciences, University of Padova, 35131 Padova, Italy;* orcid.org/0000-0001-9581-2076

Complete contact information is available at: https://pubs.acs.org/10.1021/jacs.2c05364

Notes

The authors declare no competing financial interest.

■ ACKNOWLEDGMENTS

This paper is dedicated to the memory of Prof. Armando Gennaro, a world-leading electrochemist and coinventor of electrochemically mediated ATRP, who passed away on April 13, 2022. The financial support from NSF (CHE 2000391) is gratefully acknowledged.

■ REFERENCES

(1) (a) Studer, A.; Curran, D. P. Catalysis of radical reactions: a radical chemistry perspective. *Angew. Chem., Int. Ed.* **2016**, *55* (1), 58−102. (b) Yan, M.; Lo, J. C.; Edwards, J. T.; Baran, P. S. Radicals: Reactive Intermediates with Translational Potential. *J. Am. Chem. Soc.* **2016**, *138* (39), 12692−12714. (c) Matyjaszewski, K.; Tsarevsky, N. V. Macromolecular engineering by atom transfer radical polymerization. *J. Am. Chem. Soc.* **2014**, *136* (18), 6513−6533.

(2) (a) Braunecker, W. A.; Matyjaszewski, K. Controlled/living radical polymerization: Features, developments, and perspectives. *Prog. Polym. Sci.* **2007**, *32* (1), 93−146. (b) Destarac, M. Controlled radical polymerization: industrial stakes, obstacles and achievements. *Macromol. React. Eng.* **2010**, *4* (3−4), 165−179. (c) Parkatzidis, K.; Wang, H. S.; Truong, N. P.; Anastasaki, A. Recent developments and future challenges in controlled radical polymerization: a 2020 update. *Chem.* **2020**, *6* (7), 1575−1588.

(3) (a) Matyjaszewski, K.; Xia, J. Atom transfer radical polymerization. *Chem. Rev.* **2001**, *101* (9), 2921−2990. (b) Matyjaszewski, K. Atom transfer radical polymerization (ATRP): current status and future perspectives. *Macromolecules* **2012**, *45* (10), 4015−4039.

(4) Pintauer, T.; Matyjaszewski, K. Atom transfer radical addition and polymerization reactions catalyzed by ppm amounts of copper complexes. *Chem. Soc. Rev.* **2008**, *37* (6), 1087−1097.

(5) (a) di Lena, F.; Matyjaszewski, K. Transition metal catalysts for controlled radical polymerization. *Prog. Polym. Sci.* **2010**, *35* (8),

959−1021. (b) Minisci, F. Free-radical additions to olefins in the presence of redox systems. *Acc. Chem. Res.* **1975**, *8* (5), 165−171.
(6) (a) Wang, J.-S.; Matyjaszewski, K. Controlled/″ living″ radical polymerization. atom transfer radical polymerization in the presence of transition-metal complexes. *J. Am. Chem. Soc.* **1995**, *117* (20), 5614−5615. (b) Patten, T. E.; Xia, J.; Abernathy, T.; Matyjaszewski, K. Polymers with very low polydispersities from atom transfer radical polymerization. *Science* **1996**, *272* (5263), 866−868.
(7) (a) Fischer, H. Unusual selectivities of radical reactions by internal suppression of fast modes. *J. Am. Chem. Soc.* **1986**, *108* (14), 3925−3927. (b) Daikh, B. E.; Finke, R. G. The persistent radical effect: a prototype example of extreme, 105 to 1, product selectivity in a free-radical reaction involving persistent.cntdot.CoII[macrocycle] and alkyl free radicals. *J. Am. Chem. Soc.* **1992**, *114* (8), 2938−2943. (c) Fischer, H. The persistent radical effect in controlled radical polymerizations. *J. Polym. Sci., Part A: Polym. Chem.* **1999**, *37* (13), 1885−1901.
(8) Severin, K. Ruthenium Catalysts for the Kharasch Reaction. *Curr. Org. Chem.* **2006**, *10* (2), 217−224.
(9) Reiser, O. Shining Light on Copper: Unique Opportunities for Visible-Light-Catalyzed Atom Transfer Radical Addition Reactions and Related Processes. *Acc. Chem. Res.* **2016**, *49* (9), 1990−1996.
(10) Lin, C. Y.; Coote, M. L.; Gennaro, A.; Matyjaszewski, K. Ab initio evaluation of the thermodynamic and electrochemical properties of alkyl halides and radicals and their mechanistic implications for atom transfer radical polymerization. *J. Am. Chem. Soc.* **2008**, *130* (38), 12762−12774.
(11) Isse, A. A.; Gennaro, A.; Lin, C. Y.; Hodgson, J. L.; Coote, M. L.; Guliashvili, T. Mechanism of carbon− halogen bond reductive cleavage in activated alkyl halide initiators relevant to living radical polymerization: theoretical and experimental study. *J. Am. Chem. Soc.* **2011**, *133* (16), 6254−6264.
(12) (a) Eckenhoff, W. T.; Pintauer, T. Copper catalyzed atom transfer radical addition (ATRA) and cyclization (ATRC) reactions in the presence of reducing agents. *Catal. Rev. - Sci. Eng.* **2010**, *52* (1), 1−59. (b) Ribelli, T. G.; Lorandi, F.; Fantin, M.; Matyjaszewski, K. Atom Transfer Radical Polymerization: Billion Times More Active Catalysts and New Initiation Systems. *Macromol. Rapid Commun.* **2019**, *40* (1), 1800616.
(13) (a) Tsarevsky, N. V.; Matyjaszewski, K. Green" Atom Transfer Radical Polymerization: From Process Design to Preparation of Well-Defined Environmentally Friendly Polymeric Materials. *Chem. Rev.* **2007**, *107* (6), 2270−2299. (b) Jakubowski, W.; Min, K.; Matyjaszewski, K. Activators Regenerated by Electron Transfer for Atom Transfer Radical Polymerization of Styrene. *Macromolecules* **2006**, *39* (1), 39−45.
(14) (a) Tang, W.; Kwak, Y.; Braunecker, W.; Tsarevsky, N. V.; Coote, M. L.; Matyjaszewski, K. Understanding Atom Transfer Radical Polymerization: Effect of Ligand and Initiator Structures on the Equilibrium Constants. *J. Am. Chem. Soc.* **2008**, *130* (32), 10702−10713. (b) Fang, C.; Fantin, M.; Pan, X.; de Fiebre, K.; Coote, M. L.; Matyjaszewski, K.; Liu, P. Mechanistically Guided Predictive Models for Ligand and Initiator Effects in Copper-Catalyzed Atom Transfer Radical Polymerization (Cu-ATRP). *J. Am. Chem. Soc.* **2019**, *141* (18), 7486−7497.
(15) Matyjaszewski, K.; Coca, S.; Gaynor, S. G.; Wei, M.; Woodworth, B. E. Zerovalent metals in controlled/"living" radical polymerization. *Macromolecules* **1997**, *30* (23), 7348−7350.
(16) Konkolewicz, D.; Wang, Y.; Krys, P.; Zhong, M.; Isse, A. A.; Gennaro, A.; Matyjaszewski, K. SARA ATRP or SET-lRP. end of controversy? *Polym. Chem.* **2014**, *5* (15), 4396−4417.
(17) Matyjaszewski, K.; Jakubowski, W.; Min, K.; Tang, W.; Huang, J.; Braunecker, W. A.; Tsarevsky, N. V. Diminishing catalyst concentration in atom transfer radical polymerization with reducing agents. *Proc. Natl. Acad. Sci. U.S.A.* **2006**, *103* (42), 15309−15314.
(18) (a) Eckenhoff, W. T.; Pintauer, T. Atom transfer radical addition in the presence of catalytic amounts of copper (I/II) complexes with tris (2-pyridylmethyl) amine. *Inorg. Chem.* **2007**, *46* (15), 5844−5846. (b) Taylor, M. J.; Eckenhoff, W. T.; Pintauer, T. Copper-catalyzed atom transfer radical addition (ATRA) and cyclization (ATRC) reactions in the presence of environmentally benign ascorbic acid as a reducing agent. *Dalton Trans.* **2010**, *39* (47), 11475−11482.
(19) (a) Fors, B. P.; Hawker, C. J. Control of a living radical polymerization of methacrylates by light. *Angew. Chem., Int. Ed.* **2012**, *124* (35), 8980−8983. (b) Konkolewicz, D.; Schröder, K.; Buback, J.; Bernhard, S.; Matyjaszewski, K. Visible Light and Sunlight Photoinduced ATRP with ppm of Cu Catalyst. *ACS Macro Lett.* **2012**, *1* (10), 1219−1223.
(20) Magenau, A. J.; Strandwitz, N. C.; Gennaro, A.; Matyjaszewski, K. Electrochemically mediated atom transfer radical polymerization. *Science* **2011**, *332* (6025), 81−84.
(21) (a) Mohapatra, H.; Kleiman, M.; Esser-Kahn, A. P. Mechanically controlled radical polymerization initiated by ultrasound. *Nat. Chem.* **2017**, *9* (2), 135−139. (b) Wang, Z.; Wang, Z.; Pan, X.; Fu, L.; Lathwal, S.; Olszewski, M.; Yan, J.; Enciso, A. E.; Wang, Z.; Xia, H.; Matyjaszewski, K. Ultrasonication-Induced Aqueous Atom Transfer Radical Polymerization. *ACS Macro Lett.* **2018**, *7* (3), 275−280.
(22) Pan, X.; Fantin, M.; Yuan, F.; Matyjaszewski, K. Externally controlled atom transfer radical polymerization. *Chem. Soc. Rev.* **2018**, *47* (14), 5457−5490.
(23) Dadashi-Silab, S.; Lorandi, F.; Fantin, M.; Matyjaszewski, K. Redox-switchable atom transfer radical polymerization. *Chem. Commun.* **2019**, *55* (5), 612−615.
(24) Dadashi-Silab, S.; Matyjaszewski, K. Temporal control in atom transfer radical polymerization using zerovalent metals. *Macromolecules* **2018**, *51* (11), 4250−4258.
(25) Lorandi, F.; Matyjaszewski, K. Why Do We Need More Active ATRP Catalysts? *Isr. J. Chem.* **2020**, *60* (1−2), 108−123.
(26) (a) Liarou, E.; Anastasaki, A.; Whitfield, R.; Iacono, C. E.; Patias, G.; Engelis, N. G.; Marathianos, A.; Jones, G. R.; Haddleton, D. M. Ultra-low volume oxygen tolerant photoinduced Cu-RDRP. *Polym. Chem.* **2019**, *10* (8), 963−971. (b) Theodorou, A.; Liarou, E.; Haddleton, D. M.; Stavrakaki, I. G.; Skordalidis, P.; Whitfield, R.; Anastasaki, A.; Velonia, K. Protein-polymer bioconjugates via a versatile oxygen tolerant photoinduced controlled radical polymerization approach. *Nat. Commun.* **2020**, *11* (1), 1486. (c) Liarou, E.; Whitfield, R.; Anastasaki, A.; Engelis, N. G.; Jones, G. R.; Velonia, K.; Haddleton, D. M. Copper-mediated polymerization without external deoxygenation or oxygen scavengers. *Angew. Chem., Int. Ed.* **2018**, *130* (29), 9136−9140. (d) Rolland, M.; Whitfield, R.; Messmer, D.; Parkatzidis, K.; Truong, N. P.; Anastasaki, A. Effect of polymerization components on Oxygen-Tolerant Photo-ATRP. *ACS Macro Lett.* **2019**, *8* (12), 1546−1551. (e) Matyjaszewski, K.; Dong, H.; Jakubowski, W.; Pietrasik, J.; Kusumo, A. Grafting from Surfaces for "Everyone": ARGET ATRP in the Presence of Air. *Langmuir* **2007**, *23* (8), 4528−4531.
(27) Enciso, A. E.; Fu, L.; Russell, A. J.; Matyjaszewski, K. A Breathing Atom-Transfer Radical Polymerization: Fully Oxygen-Tolerant Polymerization Inspired by Aerobic Respiration of Cells. *Angew. Chem., Int. Ed.* **2018**, *57* (4), 933−936.
(28) (a) Szczepaniak, G.; Łagodzińska, M.; Dadashi-Silab, S.; Gorczyński, A.; Matyjaszewski, K. Fully oxygen-tolerant atom transfer radical polymerization triggered by sodium pyruvate. *Chem. Sci.* **2020**, *11* (33), 8809−8816. (b) Szczepaniak, G.; Fu, L.; Jafari, H.; Kapil, K.; Matyjaszewski, K. Making ATRP More Practical: Oxygen Tolerance. *Acc. Chem. Res.* **2021**, *54* (7), 1779−1790.
(29) De Bon, F.; Fonseca, R. G.; Lorandi, F.; Serra, A. C.; Isse, A. A.; Matyjaszewski, K.; Coelho, J. F. J. The Scale-up of Electrochemically Mediated Atom Transfer Radical Polymerization without Deoxygenation. *Chem. Eng. J.* **2022**, *445*, 136690.
(30) (a) Arita, T.; Kayama, Y.; Ohno, K.; Tsujii, Y.; Fukuda, T. High-pressure atom transfer radical polymerization of methyl methacrylate for well-defined ultrahigh molecular-weight polymers. *Polymer* **2008**, *49* (10), 2426−2429. (b) Kwiatkowski, P.; Jurczak, J.; Pietrasik, J.; Jakubowski, W.; Mueller, L.; Matyjaszewski, K. High

https://doi.org/10.1021/jacs.2c05364
J. Am. Chem. Soc. XXXX, XXX, XXX−XXX

molecular weight polymethacrylates by AGET ATRP under high pressure. *Macromolecules* **2008**, *41* (4), 1067−1069.
(31) Krys, P.; Matyjaszewski, K. Kinetics of Atom Transfer Radical Polymerization. *Eur. Polym. J.* **2017**, *89*, 482−523.
(32) Fantin, M.; Isse, A. A.; Gennaro, A.; Matyjaszewski, K. Understanding the Fundamentals of Aqueous ATRP and Defining Conditions for Better Control. *Macromolecules* **2015**, *48* (19), 6862−6875.
(33) Fantin, M.; Chmielarz, P.; Wang, Y.; Lorandi, F.; Isse, A. A.; Gennaro, A.; Matyjaszewski, K. Harnessing the Interaction between Surfactant and Hydrophilic Catalyst To Control eATRP in Miniemulsion. *Macromolecules* **2017**, *50* (9), 3726−3732.
(34) Braunecker, W. A.; Tsarevsky, N. V.; Gennaro, A.; Matyjaszewski, K. Thermodynamic Components of the Atom Transfer Radical Polymerization Equilibrium: Quantifying Solvent Effects. *Macromolecules* **2009**, *42* (17), 6348−6360.
(35) (a) Ribelli, T. G.; Fantin, M.; Daran, J.-C.; Augustine, K. F.; Poli, R.; Matyjaszewski, K. Synthesis and Characterization of the Most Active Copper ATRP Catalyst Based on Tris[(4-dimethylaminopyridyl)methyl]amine. *J. Am. Chem. Soc.* **2018**, *140* (4), 1525−1534. (b) Enciso, A. E.; Lorandi, F.; Mehmood, A.; Fantin, M.; Szczepaniak, G.; Janesko, B. G.; Matyjaszewski, K. p-Substituted Tris(2-pyridylmethyl)amines as Ligands for Highly Active ATRP Catalysts: Facile Synthesis and Characterization. *Angew. Chem., Int. Ed.* **2020**, *59* (35), 14910−14920.
(36) Hansch, C.; Leo, A.; Taft, R. A survey of Hammett substituent constants and resonance and field parameters. *Chem. Rev.* **1991**, *91* (2), 165−195.
(37) Mayr, H.; Kuhn, O.; Gotta, M. F.; Patz, M. Linear free enthalpy relationships: a powerful tool for the design of organic and organometallic synthesis. *J. Phys. Org. Chem.* **1998**, *11* (8−9), 642−654.
(38) Doan, V.; Noble, B. B.; Fung, A. K. K.; Coote, M. L. Rational Design of Highly Activating Ligands for Cu-Based Atom Transfer Radical Polymerization. *J. Org. Chem.* **2019**, *84* (23), 15624−15632.
(39) Stewart, M.; Yu, L.-j.; Sherburn, M. S.; Coote, M. Computational Design of Next Generation At-om Transfer Radical Polymerization Ligands. *Polym. Chem.* **2022**, *13*, 1067−1074.
(40) Gillies, M. B.; Matyjaszewski, K.; Norrby, P.-O.; Pintauer, T.; Poli, R.; Richard, P. A DFT Study of R−X Bond Dissociation Enthalpies of Relevance to the Initiation Process of Atom Transfer Radical Polymerization. *Macromolecules* **2003**, *36* (22), 8551−8559.
(41) Lanzalaco, S.; Fantin, M.; Scialdone, O.; Galia, A.; Isse, A. A.; Gennaro, A.; Matyjaszewski, K. Atom Transfer Radical Polymerization with Different Halides (F, Cl, Br, and I): Is the Process "Living" in the Presence of Fluorinated Initiators? *Macromolecules* **2017**, *50* (1), 192−202.
(42) Gentekos, D. T.; Sifri, R. J.; Fors, B. P. Controlling polymer properties through the shape of the molecular-weight distribution. *Nat. Rev. Mater.* **2019**, *4* (12), 761−774.
(43) (a) Listak, J.; Jakubowski, W.; Mueller, L.; Plichta, A.; Matyjaszewski, K.; Bockstaller, M. R. Effect of symmetry of molecular weight distribution in block copolymers on formation of "metastable" morphologies. *Macromolecules* **2008**, *41* (15), 5919−5927. (b) Yin, R.; Wang, Z.; Bockstaller, M. R.; Matyjaszewski, K. Tuning dispersity of linear polymers and polymeric brushes grown from nanoparticles by atom transfer radical polymerization. *Polym. Chem.* **2021**, *12* (42), 6071−6082. (c) Whitfield, R.; Parkatzidis, K.; Rolland, M.; Truong, N. P.; Anastasaki, A. Tuning dispersity by photoinduced atom transfer radical polymerisation: Monomodal distributions with ppm copper concentration. *Angew. Chem., Int. Ed.* **2019**, *131* (38), 13457−13462. (d) Wang, H. S.; Parkatzidis, K.; Harrisson, S.; Truong, N. P.; Anastasaki, A. Controlling dispersity in aqueous atom transfer radical polymerization: rapid and quantitative synthesis of one-pot block copolymers. *Chem. Sci.* **2021**, *12* (43), 14376−14382. (e) Shimizu, T.; Truong, N. P.; Whitfield, R.; Anastasaki, A. Tuning Ligand Concentration in Cu (0)-RDRP: A Simple Approach to Control Polymer Dispersity. *ACS polymers Au* **2021**, *1* (3), 187−195.
(44) Dadashi-Silab, S.; Lee, I.-H.; Anastasaki, A.; Lorandi, F.; Narupai, B.; Dolinski, N. D.; Allegrezza, M. L.; Fantin, M.; Konkolewicz, D.; Hawker, C. J.; Matyjaszewski, K. Investigating Temporal Control in Photoinduced Atom Transfer Radical Polymerization. *Macromolecules* **2020**, *53* (13), 5280−5288.
(45) Barner-Kowollik, C.; Beuermann, S.; Buback, M.; Castignolles, P.; Charleux, B.; Coote, M. L.; Hutchinson, R. A.; Junkers, T.; Lacík, I.; Russell, G. T.; Stach, M.; van Herk, A. M. Critically evaluated rate coefficients in radical polymerization − 7. Secondary-radical propagation rate coefficients for methyl acrylate in the bulk. *Polym. Chem.* **2014**, *5* (1), 204−212.
(46) Fantin, M.; Isse, A. A.; Venzo, A.; Gennaro, A.; Matyjaszewski, K. Atom Transfer Radical Polymerization of Methacrylic Acid: A Won Challenge. *J. Am. Chem. Soc.* **2016**, *138* (23), 7216−7219.
(47) (a) Michieletto, A.; Lorandi, F.; De Bon, F.; Isse, A. A.; Gennaro, A. Biocompatible polymers via aqueous electrochemically mediated atom transfer radical polymerization. *J. Polym. Sci.* **2020**, *58* (1), 114−123. (b) Lorandi, F.; Fantin, M.; Wang, Y.; Isse, A. A.; Gennaro, A.; Matyjaszewski, K. Atom transfer radical polymerization of acrylic and methacrylic acids: preparation of acidic polymers with various architectures. *ACS Macro Lett.* **2020**, *9* (5), 693−699.
(48) Zhong, M.; Matyjaszewski, K. How fast can a CRP be conducted with preserved chain end functionality? *Macromolecules* **2011**, *44* (8), 2668−2677.
(49) (a) Debuigne, A.; Poli, R.; Jérôme, C.; Jérôme, R.; Detrembleur, C. Overview of cobalt-mediated radical polymerization: Roots, state of the art and future prospects. *Prog. Polym. Sci.* **2009**, *34* (3), 211−239. (b) Poli, R. A journey into metal−carbon bond homolysis. *C. R. Chim.* **2021**, *24* (1), 147−175.
(50) Wang, Y.; Soerensen, N.; Zhong, M.; Schroeder, H.; Buback, M.; Matyjaszewski, K. Improving the "livingness" of ATRP by reducing Cu catalyst concentration. *Macromolecules* **2013**, *46* (3), 683−691.
(51) (a) Fantin, M.; Lorandi, F.; Ribelli, T. G.; Szczepaniak, G.; Enciso, A. E.; Fliedel, C.; Thevenin, L.; Isse, A. A.; Poli, R.; Matyjaszewski, K. Impact of Organometallic Intermediates on Copper-Catalyzed Atom Transfer Radical Polymerization. *Macromolecules* **2019**, *52* (11), 4079−4090. (b) Zerk, T. J.; Gahan, L. R.; Krenske, E. H.; Bernhardt, P. V. The fate of copper catalysts in atom transfer radical chemistry. *Polym. Chem.* **2019**, *10* (12), 1460−1470.
(52) (a) Ribelli, T. G.; Wahidur Rahaman, S. M.; Krys, P.; Matyjaszewski, K.; Poli, R. Effect of Ligand Structure on the CuII−R OMRP Dormant Species and Its Consequences for Catalytic Radical Termination in ATRP. *Macromolecules* **2016**, *49* (20), 7749−7757. (b) Ribelli, T. G.; Augustine, K. F.; Fantin, M.; Krys, P.; Poli, R.; Matyjaszewski, K. Disproportionation or Combination? The Termination of Acrylate Radicals in ATRP. *Macromolecules* **2017**, *50* (20), 7920−7929.
(53) Francke, R.; Little, R. D.; Inagi, S. *Organic Electrosynthesis*; Wiley Online Library, 2019; Vol. 6, pp 4065−4066.
(54) (a) Chmielarz, P.; Fantin, M.; Park, S.; Isse, A. A.; Gennaro, A.; Magenau, A. J.; Sobkowiak, A.; Matyjaszewski, K. Electrochemically mediated atom transfer radical polymerization (eATRP). *Prog. Polym. Sci.* **2017**, *69*, 47−78. (b) Lorandi, F.; Fantin, M.; Isse, A. A.; Gennaro, A. Electrochemical triggering and control of atom transfer radical polymerization. *Curr. Opin. Electrochem.* **2018**, *8*, 1−7. (c) Isse, A. A.; Gennaro, A. Electrochemistry for Atom Transfer Radical Polymerization. *Chem. Rec.* **2021**, *21* (9), 2203−2222.
(55) Isse, A. A.; Visonà, G.; Ghelfi, F.; Roncaglia, F.; Gennaro, A. Electrochemical Approach to Copper-Catalyzed Reversed Atom Transfer Radical Cyclization. *Adv. Synth. Catal.* **2015**, *357* (4), 782−792.
(56) (a) Peterson, B. M.; Lin, S.; Fors, B. P. Electrochemically controlled cationic polymerization of vinyl ethers. *J. Am. Chem. Soc.* **2018**, *140* (6), 2076−2079. (b) Sang, W.; Yan, Q. Electro-Controlled Living Cationic Polymerization. *Angew. Chem., Int. Ed.* **2018**, *130* (18), 5001−5005.
(57) (a) Zhong, Y.; Feng, Q.; Wang, X.; Chen, J.; Cai, W.; Tong, R. Functionalized Polyesters via Stereoselective Electrochemical Ring-

Opening Polymerization of O-Carboxyanhydrides. *ACS Macro Lett.* **2020**, *9* (8), 1114−1118. (b) Qi, M.; Dong, Q.; Wang, D.; Byers, J. A. Electrochemically Switchable Ring-Opening Polymerization of Lactide and Cyclohexene Oxide. *J. Am. Chem. Soc.* **2018**, *140* (17), 5686−5690.

(58) (a) Lorandi, F.; Fantin, M.; Shanmugam, S.; Wang, Y.; Isse, A. A.; Gennaro, A.; Matyjaszewski, K. Toward electrochemically mediated reversible addition−fragmentation chain-transfer (e RAFT) polymerization: Can propagating radicals be efficiently electrogenerated from RAFT agents? *Macromolecules* **2019**, *52* (4), 1479−1488. (b) Strover, L. T.; Postma, A.; Horne, M. D.; Moad, G. Anthraquinone-Mediated Reduction of a Trithiocarbonate Chain-Transfer Agent to Initiate Electrochemical Reversible Addition−Fragmentation Chain Transfer Polymerization. *Macromolecules* **2020**, *53* (23), 10315−10322. (c) Wang, Y.; Fantin, M.; Park, S.; Gottlieb, E.; Fu, L.; Matyjaszewski, K. Electrochemically Mediated Reversible Addition−Fragmentation Chain-Transfer Polymerization. *Macromolecules* **2017**, *50* (20), 7872−7879.

(59) De Bon, F.; Carlan, G. M.; Tognella, E.; Isse, A. A. Exploring Electrochemically Mediated ATRP of Styrene. *Processes* **2021**, *9* (8), 1327.

(60) (a) Park, S.; Chmielarz, P.; Gennaro, A.; Matyjaszewski, K. Simplified electrochemically mediated atom transfer radical polymerization using a sacrificial anode. *Angew. Chem., Int. Ed.* **2015**, *54* (8), 2388−2392. (b) Chmielarz, P.; Sobkowiak, A.; Matyjaszewski, K. A simplified electrochemically mediated ATRP synthesis of PEO-b-PMMA copolymers. *Polymer* **2015**, *77*, 266−271.

(61) Lorandi, F.; Fantin, M.; Isse, A. A.; Gennaro, A. Electrochemically mediated atom transfer radical polymerization of n-butyl acrylate on non-platinum cathodes. *Polym. Chem.* **2016**, *7* (34), 5357−5365.

(62) (a) Yan, M.; Kawamata, Y.; Baran, P. S. Synthetic Organic Electrochemistry: Calling All Engineers. *Angew. Chem., Int. Ed.* **2018**, *57* (16), 4149−4155. (b) Zhao, B.; Mohammed, M.; Jones, B. A.; Wilson, P. Plug-and-play aqueous electrochemical atom transfer radical polymerization. *Chem. Commun.* **2021**, *57* (32), 3897−3900.

(63) Sun, Y.; Lathwal, S.; Wang, Y.; Fu, L.; Olszewski, M.; Fantin, M.; Enciso, A. E.; Szczepaniak, G.; Das, S.; Matyjaszewski, K. Preparation of Well-Defined Polymers and DNA−Polymer Bioconjugates via Small-Volume eATRP in the Presence of Air. *ACS Macro Lett.* **2019**, *8* (5), 603−609.

(64) De Bon, F.; Isse, A. A.; Gennaro, A. Towards scale-up of electrochemically-mediated atom transfer radical polymerization: Use of a stainless-steel reactor as both cathode and reaction vessel. *Electrochim. Acta* **2019**, *304*, 505−512.

(65) Magenau, A. J.; Bortolamei, N.; Frick, E.; Park, S.; Gennaro, A.; Matyjaszewski, K. Investigation of electrochemically mediated atom transfer radical polymerization. *Macromolecules* **2013**, *46* (11), 4346−4353.

(66) König, B. Photocatalysis in organic synthesis−past, present, and future. *Eur. J. Org. Chem.* **2017**, *2017* (15), 1979−1981.

(67) (a) Dadashi-Silab, S.; Atilla Tasdelen, M.; Yagci, Y. Photoinitiated atom transfer radical polymerization: Current status and future perspectives. *J. Polym. Sci., Part A: Polym. Chem.* **2014**, *52* (20), 2878−2888. (b) Pan, X.; Tasdelen, M. A.; Laun, J.; Junkers, T.; Yagci, Y.; Matyjaszewski, K. Photomediated controlled radical polymerization. *Prog. Polym. Sci.* **2016**, *62*, 73−125.

(68) (a) Ribelli, T. G.; Konkolewicz, D.; Bernhard, S.; Matyjaszewski, K. How are Radicals (Re)Generated in Photochemical ATRP? *J. Am. Chem. Soc.* **2014**, *136* (38), 13303−13312. (b) Frick, E.; Anastasaki, A.; Haddleton, D. M.; Barner-Kowollik, C. Enlightening the Mechanism of Copper Mediated PhotoRDRP via High-Resolution Mass Spectrometry. *J. Am. Chem. Soc.* **2015**, *137* (21), 6889−6896. (c) Anastasaki, A.; Nikolaou, V.; Zhang, Q.; Burns, J.; Samanta, S. R.; Waldron, C.; Haddleton, A. J.; McHale, R.; Fox, D.; Percec, V.; Wilson, P.; Haddleton, D. M. Copper(II)/Tertiary Amine Synergy in Photoinduced Living Radical Polymerization: Accelerated Synthesis of ω-Functional and α,ω-Heterofunctional Poly(acrylates). *J. Am. Chem. Soc.* **2014**, *136* (3), 1141−1149. (d) Mosnáček, J.; Ilčíková, M. Photochemically Mediated Atom Transfer Radical Polymerization of Methyl Methacrylate Using ppm Amounts of Catalyst. *Macromolecules* **2012**, *45* (15), 5859−5865.

(69) Nardi, M.; Blasco, E.; Barner-Kowollik, C. Wavelength-Resolved PhotoATRP. *J. Am. Chem. Soc.* **2022**, *144* (3), 1094−1098.

(70) (a) Yang, Q.; Dumur, F.; Morlet-Savary, F.; Poly, J.; Lalevée, J. Photocatalyzed Cu-Based ATRP Involving an Oxidative Quenching Mechanism under Visible Light. *Macromolecules* **2015**, *48* (7), 1972−1980. (b) Ma, W.; Chen, D.; Ma, Y.; Wang, L.; Zhao, C.; Yang, W. Visible-light induced controlled radical polymerization of methacrylates with Cu (dap) 2 Cl as a photoredox catalyst. *Polym. Chem.* **2016**, *7* (25), 4226−4236. (c) Yang, Q.; Lalevée, J.; Poly, J. Development of a Robust Photocatalyzed ATRP Mechanism Exhibiting Good Tolerance to Oxygen and Inhibitors. *Macromolecules* **2016**, *49* (20), 7653−7666.

(71) Treat, N. J.; Fors, B. P.; Kramer, J. W.; Christianson, M.; Chiu, C.-Y.; Read de Alaniz, J.; Hawker, C. J. Controlled radical polymerization of acrylates regulated by visible light. *ACS Macro Lett.* **2014**, *3* (6), 580−584.

(72) (a) Treat, N. J.; Sprafke, H.; Kramer, J. W.; Clark, P. G.; Barton, B. E.; Read de Alaniz, J.; Fors, B. P.; Hawker, C. J. Metal-free atom transfer radical polymerization. *J. Am. Chem. Soc.* **2014**, *136* (45), 16096−16101. (b) Corbin, D. A.; Miyake, G. M. Photoinduced Organocatalyzed Atom Transfer Radical Polymerization (O-ATRP): Precision Polymer Synthesis Using Organic Photoredox Catalysis. *Chem. Rev.* **2022**, *122* (2), 1830−1874. (c) Du, Y.; Pearson, R. M.; Lim, C. H.; Sartor, S. M.; Ryan, M. D.; Yang, H.; Damrauer, N. H.; Miyake, G. M. Strongly reducing, visible-light organic photoredox catalysts as sustainable alternatives to precious metals. *Chem.—Eur. J.* **2017**, *23* (46), 10962−10968. (d) Singh, V. K.; Yu, C.; Badgujar, S.; Kim, Y.; Kwon, Y.; Kim, D.; Lee, J.; Akhter, T.; Thangavel, G.; Park, L. S. Highly efficient organic photocatalysts discovered via a computer-aided-design strategy for visible-light-driven atom transfer radical polymerization. *Nat. Catal.* **2018**, *1* (10), 794−804. (e) Theriot, J. C.; Lim, C.-H.; Yang, H.; Ryan, M. D.; Musgrave, C. B.; Miyake, G. M. Organocatalyzed atom transfer radical polymerization driven by visible light. *Science* **2016**, *352* (6289), 1082−1086.

(73) Kutahya, C.; Aykac, F. S.; Yilmaz, G.; Yagci, Y. LED and visible light-induced metal free ATRP using reducible dyes in the presence of amines. *Polym. Chem.* **2016**, *7* (39), 6094−6098.

(74) Staveness, D.; Bosque, I.; Stephenson, C. R. J. Free Radical Chemistry Enabled by Visible Light-Induced Electron Transfer. *Acc. Chem. Res.* **2016**, *49* (10), 2295−2306.

(75) (a) Arceo, E.; Montroni, E.; Melchiorre, P. Photo-Organocatalysis of Atom-Transfer Radical Additions to Alkenes. *Angew. Chem., Int. Ed.* **2014**, *53* (45), 12064−12068. (b) Ravelli, D.; Fagnoni, M. Aromatic Aldehydes as Energy-Transfer Photoorganocatalysts. *ChemCatChem.* **2015**, *7* (5), 735−737.

(76) Pan, X.; Fang, C.; Fantin, M.; Malhotra, N.; So, W. Y.; Peteanu, L. A.; Isse, A. A.; Gennaro, A.; Liu, P.; Matyjaszewski, K. Mechanism of Photoinduced Metal-Free Atom Transfer Radical Polymerization: Experimental and Computational Studies. *J. Am. Chem. Soc.* **2016**, *138* (7), 2411−2425.

(77) Theriot, J. C.; McCarthy, B. G.; Lim, C.-H.; Miyake, G. M. Organocatalyzed Atom Transfer Radical Polymerization: Perspectives on Catalyst Design and Performance. *Macromol. Rapid Commun.* **2017**, *38* (13), 1700040.

(78) Corbin, D. A.; McCarthy, B. G.; van de Lindt, Z.; Miyake, G. M. Radical cations of phenoxazine and dihydrophenazine photoredox catalysts and their role as deactivators in organocatalyzed atom transfer radical polymerization. *Macromolecules* **2021**, *54* (10), 4726−4738.

(79) (a) Mansour, M.; Giacovazzi, R.; Ouali, A.; Taillefer, M.; Jutand, A. Activation of aryl halides by Cu 0/1, 10-phenanthroline: Cu 0 as precursor of Cu I catalyst in cross-coupling reactions. *Chem. Commun.* **2008**, No. 45, 6051−6053. (b) Bortolato, T.; Cuadros, S.; Simionato, G.; Dell'Amico, L. The advent and development of organophotoredox catalysis. *Chem. Commun.* **2022**, *58* (9), 1263−1283. (c) Engl, S.; Reiser, O. Making Copper Photocatalysis Even

https://doi.org/10.1021/jacs.2c05364
J. Am. Chem. Soc. XXXX, XXX, XXX−XXX

More Robust and Economic: Photoredox Catalysis with [CuII(dmp)-2Cl]Cl. *Eur. J. Org. Chem.* **2020**, *2020* (10), 1523−1533.
(80) Rawner, T.; Lutsker, E.; Kaiser, C. A.; Reiser, O. The different faces of photoredox catalysts: visible-light-mediated atom transfer radical addition (ATRA) reactions of perfluoroalkyl iodides with styrenes and phenylacetylenes. *ACS Catal.* **2018**, *8* (5), 3950−3956.
(81) Wu, C.; Corrigan, N.; Lim, C.-H.; Liu, W.; Miyake, G.; Boyer, C. Rational Design of Photocatalysts for Controlled Polymerization: Effect of Structures on Photocatalytic Activities. *Chem. Rev.* **2022**, *122* (6), 5476−5518.
(82) McCarthy, B.; Sartor, S.; Cole, J.; Damrauer, N.; Miyake, G. M. Solvent Effects and Side Reactions in Organocatalyzed Atom Transfer Radical Polymerization for Enabling the Controlled Polymerization of Acrylates Catalyzed by Diaryl Dihydrophenazines. *Macromolecules* **2020**, *53* (21), 9208−9219.
(83) Buss, B. L.; Lim, C.-H.; Miyake, G. M. Dimethyl Dihydroacridines as Photocatalysts in Organocatalyzed Atom Transfer Radical Polymerization of Acrylate Monomers. *Angew. Chem., Int. Ed.* **2020**, *59* (8), 3209−3217.
(84) Corbin, D. A.; McCarthy, B. G.; Miyake, G. M. Impacts of performing electrolysis during organocatalyzed atom transfer radical polymerization. *Polym. Chem.* **2020**, *11* (31), 4978−4985.
(85) Corbin, D. A.; Puffer, K. O.; Chism, K. A.; Cole, J. P.; Theriot, J. C.; McCarthy, B. G.; Buss, B. L.; Lim, C.-H.; Lincoln, S. R.; Newell, B. S. Radical addition to N, N-diaryl dihydrophenazine photoredox catalysts and implications in photoinduced organocatalyzed atom transfer radical polymerization. *Macromolecules* **2021**, *54* (10), 4507−4516.
(86) Kütahya, C.; Schmitz, C.; Strehmel, V.; Yagci, Y.; Strehmel, B. Near-Infrared Sensitized Photoinduced Atom-Transfer Radical Polymerization (ATRP) with a Copper (II) Catalyst Concentration in the ppm Range. *Angew. Chem., Int. Ed.* **2018**, *57* (26), 7898−7902.
(87) Zhang, W.; He, J.; Lv, C.; Wang, Q.; Pang, X.; Matyjaszewski, K.; Pan, X. Atom transfer radical polymerization driven by near-infrared light with recyclable upconversion nanoparticles. *Macromolecules* **2020**, *53* (12), 4678−4684.
(88) (a) Kütahya, C.; Wang, P.; Li, S.; Liu, S.; Li, J.; Chen, Z.; Strehmel, B. Carbon dots as a promising green photocatalyst for free radical and ATRP-based radical photopolymerization with blue LEDs. *Angew. Chem., Int. Ed.* **2020**, *59* (8), 3166−3171. (b) Kütahya, C.; Zhai, Y.; Li, S.; Liu, S.; Li, J.; Strehmel, V.; Chen, Z.; Strehmel, B. Distinct Sustainable Carbon Nanodots Enable Free Radical Photopolymerization, Photo-ATRP and Photo-CuAAC Chemistry. *Angew. Chem., Int. Ed.* **2021**, *60* (19), 10983−10991. (c) Lu, Z.; Fu, X.; Yang, H.; Zhao, Y.; Xiao, L.; Hou, L. A covalent organic framework as a photocatalyst for atom transfer radical polymerization under white light irradiation. *Polym. Chem.* **2021**, *12* (2), 183−188. (d) Sun, M.; Lorandi, F.; Yuan, R.; Dadashi-Silab, S.; Kowalewski, T.; Matyjaszewski, K. Assemblies of Polyacrylonitrile-Derived Photoactive Polymers as Blue and Green Light Photo-Cocatalysts for Cu-Catalyzed ATRP in Water and Organic Solvents. *Front. Chem.* **2021**, *9*, 734076. (e) Dadashi-Silab, S.; Kim, K.; Lorandi, F.; Szczepaniak, G.; Kramer, S.; Peteanu, L.; Matyjaszewski, K. Red-Light-Induced, Copper-Catalyzed Atom Transfer Radical Polymerization. *ACS Macro Lett.* **2022**, *11* (3), 376−381.
(89) Qiao, L.; Zhou, M.; Shi, G.; Cui, Z.; Zhang, X.; Fu, P.; Liu, M.; Qiao, X.; He, Y.; Pang, X. Ultrafast Visible-Light-Induced ATRP in Aqueous Media with Carbon Quantum Dots as the Catalyst and Its Application for 3D Printing. *J. Am. Chem. Soc.* **2022**, *144* (22), 9817−9826.
(90) Qiao, X.; Hao, Q.; Chen, M.; Shi, G.; He, Y.; Pang, X. Simple Full-Spectrum Heterogeneous Photocatalyst for Photo-induced Atom Transfer Radical Polymerization (ATRP) under UV/vis/NIR and its Application for the Preparation of Dual Mode Curing Injectable Photoluminescence Hydrogel. *ACS Appl. Mater. Interfaces* **2022**, *14* (18), 21555−21563.
(91) (a) An, Z.; Zhu, S.; An, Z. Heterogeneous photocatalytic reversible deactivation radical polymerization. *Polym. Chem.* **2021**, *12* (16), 2357−2373. (b) Dadashi-Silab, S.; Lorandi, F.; DiTucci, M. J.; Sun, M.; Szczepaniak, G.; Liu, T.; Matyjaszewski, K. Conjugated cross-linked phenothiazines as green or red light heterogeneous photocatalysts for copper-catalyzed atom transfer radical polymerization. *J. Am. Chem. Soc.* **2021**, *143* (25), 9630−9638.
(92) Chen, M.; Deng, S.; Gu, Y.; Lin, J.; MacLeod, M. J.; Johnson, J. A. Logic-controlled radical polymerization with heat and light: multiple-stimuli switching of polymer chain growth via a recyclable, thermally responsive gel photoredox catalyst. *J. Am. Chem. Soc.* **2017**, *139* (6), 2257−2266.
(93) Shanmugam, S.; Xu, J.; Boyer, C. Exploiting Metalloporphyrins for Selective Living Radical Polymerization Tunable over Visible Wavelengths. *J. Am. Chem. Soc.* **2015**, *137* (28), 9174−9185.
(94) Corrigan, N.; Rosli, D.; Jones, J. W. J.; Xu, J.; Boyer, C. Oxygen tolerance in living radical polymerization: investigation of mechanism and implementation in continuous flow polymerization. *Macromolecules* **2016**, *49* (18), 6779−6789.
(95) (a) Li, J.; Nagamani, C.; Moore, J. S. Polymer Mechanochemistry: From Destructive to Productive. *Acc. Chem. Res.* **2015**, *48* (8), 2181−2190. (b) Krusenbaum, A.; Grätz, S.; Tigineh, G. T.; Borchardt, L.; Kim, J. G. The mechanochemical synthesis of polymers. *Chem. Soc. Rev.* **2022**, *51*, 2873−2905.
(96) Wang, Z.; Pan, X.; Yan, J.; Dadashi-Silab, S.; Xie, G.; Zhang, J.; Wang, Z.; Xia, H.; Matyjaszewski, K. Temporal control in mechanically controlled atom transfer radical polymerization using low ppm of Cu catalyst. *ACS Macro Lett.* **2017**, *6* (5), 546−549.
(97) Zhou, Y.-N.; Li, J.-J.; Ljubic, D.; Luo, Z.-H.; Zhu, S. Mechanically mediated atom transfer radical polymerization: Exploring its potential at high conversions. *Macromolecules* **2018**, *51* (17), 6911−6921.
(98) Wang, Z.; Pan, X.; Li, L.; Fantin, M.; Yan, J.; Wang, Z.; Wang, Z.; Xia, H.; Matyjaszewski, K. Enhancing mechanically induced ATRP by promoting interfacial electron transfer from piezoelectric nanoparticles to Cu catalysts. *Macromolecules* **2017**, *50* (20), 7940−7948.
(99) (a) McKenzie, T. G.; Colombo, E.; Fu, Q.; Ashokkumar, M.; Qiao, G. G. Sono-RAFT polymerization in aqueous medium. *Angew. Chem., Int. Ed.* **2017**, *56* (40), 12302−12306. (b) Wang, Z.; Wang, Z.; Pan, X.; Fu, L.; Lathwal, S.; Olszewski, M.; Yan, J.; Enciso, A. E.; Wang, Z.; Xia, H. Ultrasonication-induced aqueous atom transfer radical polymerization. *ACS Macro Lett.* **2018**, *7* (3), 275−280.
(100) Wang, Z.; Lorandi, F.; Fantin, M.; Wang, Z.; Yan, J.; Wang, Z.; Xia, H.; Matyjaszewski, K. Atom transfer radical polymerization enabled by sonochemically labile Cu-carbonate species. *ACS Macro Lett.* **2019**, *8* (2), 161−165.
(101) Cho, H. Y.; Bielawski, C. W. Atom Transfer Radical Polymerization in the Solid-State. *Angew. Chem., Int. Ed.* **2020**, *132* (33), 14033−14039.
(102) Schumacher, C.; Hernández, J. G.; Bolm, C. Electromechanochemical atom transfer radical cyclizations using piezoelectric BaTiO3. *Angew. Chem., Int. Ed.* **2020**, *59* (38), 16357−16360.
(103) Martinez, M. R.; Sobieski, J.; Lorandi, F.; Fantin, M.; Dadashi-Silab, S.; Xie, G.; Olszewski, M.; Pan, X.; Ribelli, T. G.; Matyjaszewski, K. Understanding the relationship between catalytic activity and termination in photoATRP: Synthesis of linear and bottlebrush polyacrylates. *Macromolecules* **2020**, *53* (1), 59−67.
(104) Szczepaniak, G.; Piątkowski, J.; Nogaś, W.; Lorandi, F.; Yerneni, S. S.; Fantin, M.; Ruszczyńska, A.; Enciso, A. E.; Bulska, E.; Grela, K. An isocyanide ligand for the rapid quenching and efficient removal of copper residues after Cu/TEMPO-catalyzed aerobic alcohol oxidation and atom transfer radical polymerization. *Chem. Sci.* **2020**, *11* (16), 4251−4262.
(105) (a) Simakova, A.; Mackenzie, M.; Averick, S. E.; Park, S.; Matyjaszewski, K. Bioinspired Iron-Based Catalyst for Atom Transfer Radical Polymerization. *Angew. Chem., Int. Ed.* **2013**, *52* (46), 12148−12151. (b) Teodorescu, M.; Gaynor, S. G.; Matyjaszewski, K. Halide anions as ligands in iron-mediated atom transfer radical polymerization. *Macromolecules* **2000**, *33* (7), 2335−2339. (c) Dadashi-Silab, S.; Matyjaszewski, K. Iron Catalysts in Atom Transfer Radical Polymerization. *Molecules* **2020**, *25* (7), 1648.

https://doi.org/10.1021/jacs.2c05364
J. Am. Chem. Soc. XXXX, XXX, XXX−XXX

(106) Dworakowska, S.; Lorandi, F.; Gorczyński, A.; Matyjaszewski, K. Toward Green Atom Transfer Radical Polymerization: Current Status and Future Challenges. *Adv. Sci.* **2022**, *9* (19), 2106076.

(107) Thevenin, L.; Fliedel, C.; Matyjaszewski, K.; Poli, R. Impact of Catalyzed Radical Termination (CRT) and Reductive Radical Termination (RRT) in Metal-Mediated Radical Polymerization Processes. *Eur. J. Inorg. Chem.* **2019**, *2019* (42), 4489−4499.

(108) (a) Wang, Y.; Zhang, Y.; Parker, B.; Matyjaszewski, K. ATRP of MMA with ppm levels of iron catalyst. *Macromolecules* **2011**, *44* (11), 4022−4025. (b) Dadashi-Silab, S.; Kim, K.; Lorandi, F.; Schild, D. J.; Fantin, M.; Matyjaszewski, K. Effect of halogen and solvent on iron-catalyzed atom transfer radical polymerization. *Polym. Chem.* **2022**, *13* (8), 1059−1066.

(109) De Bon, F.; Ribeiro, D. C.; Abreu, C. M.; Rebelo, R. A.; Isse, A. A.; Serra, A. C.; Gennaro, A.; Matyjaszewski, K.; Coelho, J. F. Under pressure: electrochemically-mediated atom transfer radical polymerization of vinyl chloride. *Polym. Chem.* **2020**, *11* (42), 6745−6762.

(110) Kaneyoshi, H.; Inoue, Y.; Matyjaszewski, K. Synthesis of block and graft copolymers with linear polyethylene segments by combination of degenerative transfer coordination polymerization and atom transfer radical polymerization. *Macromolecules* **2005**, *38* (13), 5425−5435.

(111) (a) Nicolaÿ, R.; Kwak, Y.; Matyjaszewski, K. A Green Route to Well-Defined High-Molecular-Weight (Co) polymers Using ARGET ATRP with Alkyl Pseudohalides and Copper Catalysis. *Angew. Chem., Int. Ed.* **2010**, *122* (3), 551−554. (b) Kwak, Y.; Nicolaÿ, R.; Matyjaszewski, K. Synergistic interaction between ATRP and RAFT: taking the best of each world. *Aust. J. Chem.* **2009**, *62* (11), 1384−1401.

(112) (a) Barham, J. P.; König, B. Synthetic photoelectrochemistry. *Angew. Chem., Int. Ed.* **2020**, *59* (29), 11732−11747. (b) Liu, J.; Lu, L.; Wood, D.; Lin, S. New Redox Strategies in Organic Synthesis by Means of Electrochemistry and Photochemistry. *ACS Central Sci.* **2020**, *6* (8), 1317−1340.

(113) (a) Matyjaszewski, K. Advanced materials by atom transfer radical polymerization. *Adv. Mater.* **2018**, *30* (23), 1706441. (b) Matyjaszewski, K.; Spanswick, J. Controlled/living radical polymerization. *Mater. Today* **2005**, *8* (3), 26−33.

(114) (a) Martinez, M. R.; Dadashi-Silab, S.; Lorandi, F.; Zhao, Y.; Matyjaszewski, K. Depolymerization of P(PDMS11MA) Bottlebrushes via Atom Transfer Radical Polymerization with Activator Regeneration. *Macromolecules* **2021**, *54* (12), 5526−5538. (b) Martinez, M. R.; De Luca Bossa, F.; Olszewski, M.; Matyjaszewski, K. Copper(II) Chloride/Tris(2-pyridylmethyl)amine-Catalyzed Depolymerization of Poly(n-butyl methacrylate). *Macromolecules* **2022**, *55* (1), 78−87.

(115) Yan, J.; Bockstaller, M. R.; Matyjaszewski, K. Brush-modified materials: Control of molecular architecture, assembly behavior, properties and applications. *Prog. Polym. Sci.* **2020**, *100*, 101180.

(116) Xie, G.; Martinez, M. R.; Olszewski, M.; Sheiko, S. S.; Matyjaszewski, K. Molecular Bottlebrushes as Novel Materials. *Biomacromolecules* **2019**, *20* (1), 27−54.

(117) Baker, S. L.; Kaupbayeva, B.; Lathwal, S.; Das, S. R.; Russell, A. J.; Matyjaszewski, K. Atom Transfer Radical Polymerization for Biorelated Hybrid Materials. *Biomacromolecules* **2019**, *20* (12), 4272−4298.

(118) (a) Romio, M.; Trachsel, L.; Morgese, G.; Ramakrishna, S. N.; Spencer, N. D.; Benetti, E. M. Topological Polymer Chemistry Enters Materials Science: Expanding the Applicability of Cyclic Polymers. *ACS Macro Lett.* **2020**, *9* (7), 1024−1033. (b) Banquy, X.; Burdynska, J.; Lee, D. W.; Matyjaszewski, K.; Israelachvili, J. Bioinspired bottlebrush polymer exhibits low friction and Amontons-like behavior. *J. Am. Chem. Soc.* **2014**, *136* (17), 6199−6202.

https://doi.org/10.1021/jacs.2c05364
J. Am. Chem. Soc. XXXX, XXX, XXX−XXX